Russian Chemical Reviews **80** (10) 971 – 991 (2011) © 2011 Russian Academy of Sciences and Turpion Ltd

DOI 10.1070/RC2011v080n10ABEH004176

Gas hydrates: nanosized phases in the separation and purification of substances by crystallization

V M Vorotyntsev, V M Malyshev

Contents

I.	Introduction	971
II.	The structures of gas hydrates and physicochemical models for their formation	972
III.	Separation of gaseous components during gas hydrate crystallization	975
IV.	High purification of fluorides by the gas hydrate crystallization method	986
V.	Conclusion	988

Abstract. Structural features of the nanosized phases of gas hydrates are considered. Physicochemical models for the formation of these phases are analyzed. Mathematical models for high purification of gases by gas hydrate crystallization and an algorithm for calculations of the parameters affecting the purification efficiency are given. Procedures for calculations of the distribution coefficients of mixture components between phases during the formation of mixed gas hydrates are discussed. The bibliography includes 109 references.

I. Introduction

Gas hydrates are key process components in the gas and petroleum industries. The formation of gas hydrates can significantly change the conditions for gas and oil production, in particular, cause emergency situations. At the same time, of considerable interest is the treatment of gas hydrates as nanosized phases in the separation and purification of gas mixtures including production and transportation of natural gas.[1] Research on these processes will help to determine the chemical compositions of gas mixtures and conditions suitable for avoiding the formation of gas hydrates and related emergency situations.

At present, there are severe requirements on the purity of process gases for industrial purposes. Therefore, elaboration of new and improvement of the known methods of purification are topical. Isomorphous co-precipitation of substances in the form of gas hydrates[2] called gas hydrate crystallization[3] is a promising technique for separation and purification of gas mixtures. Gas hydrate crystallization can occur at about 0 °C under low pressures. It is a highly efficient, safe and environmentally friendly method for separation and purification of gas mixtures which requires relatively low energy expenditure compared to conventional methods.

Recently, a number of reviews have been reported,[3–6] concerning some historical details and physicochemical properties of gas hydrates. The kinetics of formation, morphology, thermodynamics and properties of gas hydrates were discussed at the Third (USA, 1999), Fourth (Japan, 2002), Fifth (Norway, 2005) and Sixth (Canada, 2008) International Conferences on gas hydrates. A total of 650 communications submitted to the Seventh International Conference on gas hydrates (United Kingdom, 2011) indicate intensive progress in this field. Of course, most studies were devoted to natural gas hydrates; the number of communications on the use of gas hydrates for separation of gas components was much smaller.

The separation process is based on the difference between the chemical compositions and properties of solid and liquid (or gas) phases. In the course of gas hydrate crystallization, components of a gas mixture are redistributed between the gas and solid (gas hydrate) phases. It was proposed to characterize the ability of gas hydrates to maintain compositional difference between the equilibrium gas and solid phases by the Berthelot – Nernst distribution constant (coefficient) and to use this parameter for separation and concentration of noble gases and natural gas components.[2,7]

The unit cells in the crystal framework of a gas hydrate are 1 – 2 nm in size. A statistically valuable phase formation (including at least 1000 unit cells) has a size ranging from 15 to 20 nm. This allows gas hydrates to be treated as a nanosized phase in biphasic methods of separation and high purification of substances. Of considerable interest is analysis of the chemical compositions of such phases and evaluation of the efficiency of gas hydrate methods for high purification of gas.[3]

In this review, we analyze modern physicochemical models for gas hydrate formation and algorithms for calculating the distribution coefficients of gas mixture components between the gas and solid phases based on

V M Vorotyntsev, V M Malyshev R E Alekseev Nizhnii Novgorod State Technical University, ul. Minina 24, 603950 Nizhnii Novgorod, Russian Federation. Fax/tel. (7-831) 436 03 61, e-mail: vlad@vorotyn.nnov.ru

Received 20 July 2010
Uspekhi Khimii **80** (10) 1013 – 1033 (2011); translated by A M Raevskiy

these models. We will also consider mathematical models for separation and high purification of gas by gas hydrate crystallization and evaluate their efficiency taking purification of sulfur hexafluoride and carbon tetrafluoride as examples.

II. The structures of gas hydrates and physicochemical models for their formation

1. The structures of gas hydrates

Gas hydrates are solid crystalline substances of variable composition belonging to clathrates. The chemical composition of gas hydrates is described by the general formula $M \cdot n\,H_2O$, where M is the molecule of the hydrate-forming gas at a specified temperature and pressure and n is the hydrate number dependent on the nature of the hydrate-forming gas, pressure and temperature.

There exist individual, double and mixed hydrates. The chemical composition of mixed hydrates includes a number of gases. To date, more than 150 substances capable of forming gas hydrates are known.[8] This property has found practical applications in, *e.g.*, concentration of heavy water and thermal compression of gases,[9–10] demineralization and separation of salt solutions,[11–15] for container transportation of natural gas and storage of gases in the form of hydrates.[6–18] Most gas hydrates known to date form three types of crystal structures, *viz.*, structures I, II and H with the cubic (space group $Pm3n$, $Fd3m$) and hexagonal (space group $P6/mmm$) symmetry, respectively. These structures include five fundamental types of cavities in the crystal framework.

The results of studies on high-pressure gas phases suggest the existence of gas hydrates with some other structures.[19–22] For instance, a new argon hydrate structure was reported[22] and a fourth structural type of gas hydrates (space group $P4_2/mnm$) identified in gas-phase neutron diffraction studies of high-pressure gas hydrate phases in the systems argon–water and tetrahydrofuran–water was discovered.[23] Selected parameters of the crystal structures of gas hydrates were also considered.[3,24]

It was experimentally shown that large cavities of hydrates with the type-I and type-II structures can house two nitrogen molecules.[25] Hydrates with the cubic structure II and small guest molecules are more stable than the hydrates with the type-I structure. The cubic structure I is more favourable for the hydrates containing larger molecules (H_2S, Xe, *etc.*) that cannot be accommodated two at a time within the same cavity. Also, large cavities of the structure-II hydrates can house two molecules of such gases as oxygen, nitrogen, krypton and argon.[26]

2. The kinetics of formation, growth and decomposition of gas hydrates

To use gas hydrates for separation of gas mixtures, one should have complete information on the structure of hydrates and mechanism of their formation. Most difficult is to study the kinetics of hydrate formation. This is first of all due to the fact that a hydrate can form in the reaction

$$M + n\,H_2O \rightleftharpoons [M \cdot n\,H_2O]_{hydr}$$

under different conditions.

The nucleation and growth of gas hydrate crystals can occur:

— at the water(ice)/gas interface;

— in the bulk of free gas saturated with water vapours; and

— in the bulk of gas-saturated water.

In each case, the nucleation mechanism of gas hydrates has its own features.[24,27–32] For instance, the morphology of hydrate crystals was studied and factors affecting the rates of their nucleation and growth were reported.[28] It was established that the rate of hydrate formation depends on the degree of supercooling of the solution, on the pressure, temperature, phase state of water and on the chemical composition of the gas-hydrate-forming gas. A model for hydrate formation with one fitting parameter was developed.[31] It is based on the theory of homogeneous crystallization and treats the growth of a hydrate crystal as two-step process. It was shown that hydrates can form not only within a thin layer at the gas/water interface,[33] but also in the bulk of the liquid phase. The model[34] for gas hydrate formation allows one to take account of heat transfer effects. The model of nonreacting compressible nucleus[35] describes the kinetics of formation of gas hydrate from ice. A method for numerical solution of kinetic equations for this case was developed. Experiments on the formation of carbon dioxide and methane gas hydrates carried out to verify the model confirmed its applicability.

Limitations on the possibility of direct observation (nanoscale particle size), the influence of heat and mass transfer as well as difficulties in the isolation and exact determination of the amount of hydrate formed preclude obtaining of reliable experimental data on the formation and decomposition of gas hydrates. Therefore, the results of determination of the dissociation pressure, parameters of quadrupole points in phase diagrams and the compositions of gas hydrates reported by different authors are different.

Experimental difficulties can be avoided using molecular modeling methods.[36]

3. The model of ideal solid clathrate

To describe the nonstoichiometric nature of clathrate crystals, a model of ideal solutions was proposed.[37] It assumes the same type for all cavities and a single type of guest molecules. Taking into account specific features of gas hydrates (presence of large and small cavities in the type-I and type-II structures, water crystal framework, *etc.*) required significant modification of the equations. This was done elsewhere.[38] There is also a model of clathrates with different types of cavities and different types of guest molecules.[39] It is called 'the model of ideal solid clathrate'.

The theory of ideal solid clathrates is based on the similarity between hydrate formation and physisorption and on the Lennard–Jones and Devonshire model for the structure of fluids.[40]

The model of 'ideal solid clathrate' assumes that

— energies of host molecules are independent of the energies of guest molecules;

— nonpolar guest molecules fill cavities that can house at most one molecule each;

— guest molecules in cavities obey classical statistics; and

— guest–guest interaction is negligible.

From the model of ideal clathrate it follows that, assuming equilibrium distribution of guest molecules in the gas hydrate cavities, the chemical potential of water molecules has the form[38,39]

$$\mu_w = \mu_w^0 + kT\sum_i n_i \ln(1 - Q_i), \quad (1)$$

where μ_w^0 is the chemical potential of the empty hydrate framework, n_i is the ratio of the number of cavities of the ith type in the unit cell to the number of water molecules forming the cell, and Q_i is the proportion of gas-filled cavities. The parameter Q_i is given by the known expression for the Langmuir adsorption isotherm

$$Q_i = \frac{C_i f_i}{1 + C_i f_i}. \quad (2)$$

Here C_i is the Langmuir coefficient of the ith gas, which depends on the temperature and pressure (although weakly), and f_i is the fugacity of molecules of the ith gas [41] (it can be determined from the Redlich–Kwong equation of state [42] with a reasonable accuracy).

Using Eqn (1), one can determine the minimum proportion of filled cavities while Eqn (2) provides the minimum pressure of the ith gas (dissociation pressure) necessary to stabilize the hydrate at a given temperature.

The maximum pressures at which gas hydrates are still stable lie between 15 000 and 20 000 atm.[43–45]

Provided that a gas hydrate is in thermodynamic equilibrium with water vapour, the saturated vapour pressure above the surface of the gas hydrate is given by [38]

$$P_w = P_w^0 - \sum_i n_i \ln(1 + C_i f_i), \quad (3)$$

where P_w^0 is the saturated vapour pressure above the empty clathrate framework, which depends on the temperature and structural type of the hydrate. Using experimental data for the best studied methane hydrate (structure I) and propane hydrate (structure II), it was shown [27] that the dependences $P_w^{0(I,II)}$ are described in the temperature range 260–290 K with a reasonable accuracy (deviation is about 3.5%) by the following equations:

$$\ln P_w^{0(I)} = -128.0009 + 22.0937 \ln T - \frac{193.6439}{T}, \quad (4a)$$

$$\ln P_w^{0(II)} = -111.0433 + 20.2241 \ln T - \frac{690.3979}{T}. \quad (4b)$$

Thus, Eqns (3) and (4) allow one to calculate the dissociation pressure (or fugacity) of a gas hydrate or the saturated water vapour pressure above the gas hydrate surface if the Langmuir coefficients are known.

The assumptions made in constructing the model of ideal clathrate solutions are similar to those used in models of ideal solutions. Correspondingly, both types of models have identical fields of application. They can be used either at very low impurity concentrations (weak guest–guest interaction) or if the solute molecules weakly interact with one another. Clearly, the first condition is not met in clathrate systems. Guest molecules are reasonably close to one another and, if the energy of the guest–guest interaction is high enough, the mutual influence of the guest molecules is significant. It should be noted that improved models for the description of gas hydrates based on statistical thermodynamics laws are developed.[24, 46–48]

4. The model of nonideal solid clathrate

Thermodynamic description of gas hydrates can be improved using the model of regular solution instead of the model of ideal solution. The model thus obtained is called 'the model of regular solid clathrate'.

An attempt to calculate the statistical sum for a clathrate taking account of the interaction between guest molecules was reported.[49] The guest–guest interaction treated as 'addtive' to the host–guest interaction was taken into account by adding the potential of guest molecules located at the centres of the neighbouring cavities to the cell host potential. Unlike Ref. 49, the authors of Refs 50–53 considered the guest–guest interaction as 'having equal rights' with the host–guest interaction rather than an 'additive'. It is believed that the guest–guest interaction is the weakest interaction in clathrate systems. However, it significantly influences the stoichiometry of clathrates [54] and, to a lesser extent, their stability. Taking account of guest–guest interaction allows one to describe various phase transitions in systems.

As applied to gas hydrates, the thermodynamic model of regular clathrate is characterized by the following key admissions:[24]

— each cavity can hold only one gas molecule and some cavities remain unfilled; same-type cavities are thermodynamically equivalent;

— molecules in cavities execute nearly free rotation; thus, the motion of the centre of mass of the guest molecule and rotation of the entire guest molecule are almost independent;

— the interaction between guest molecules located in the neighbouring cavities is taken into account; this interaction has no effect on the random character of the distribution of gas molecules over cavities;

— the free energy of hydrate is the additive sum of the free energies of water framework and guest molecules.

In this model, the chemical potentials of water and 'guest molecules are determined using expressions similar to Eqns (1) and (3) augmented with the term taking account of the guest–guest interaction. The second admission allows one to describe this interaction by a temperature-independent coefficient. The Langmuir coefficients and the chemical potentials of water molecules calculated using the models of ideal and regular solid clathrate differ appreciably.[55]

The model of regular solid clathrate was improved.[56] It was assumed that, when calculating the dissociation pressure of gas hydrates taking into account the guest–guest interaction, the magnitude of this interaction depends on the guest molecules. The authors of Ref. 56 believed that the guest molecule should first of all distort the water framework, although other factors, *e.g.*, polarity of the guest molecule, also can affect its parameters. The experimentally substantiated values μ_w^0 for each gas hydrate depend on the nature of the guest molecule and increase with the guest volume. When calculating the dissociation pressure, the use of reference data on the properties of all molecules decreases the error.

It should be emphasized that at high degrees of filling of cavities in the hydrate framework and at close values of the guest–guest interaction parameters for different gases (when considering narrow groups of gas mixtures, *e.g.*, natural gas, hydrides, fluorides, *etc.*), the contributions to

the corresponding expressions are almost the same and independent of the chemical composition of the gas phase. In this case, the guest–guest interaction can formally be included in μ_w^0 (Ref. 24). That is why the field of application of the model of ideal gas hydrate extends considerably.

In the cell potential method,[57] the potential of the host–guest interaction in clathrate hydrates is calculated analytically. The technique allows one to determine parameters of the potential interaction for hydrates with the known Langmuir coefficients. It was used to calculate parameters of a number of structural transitions in gas hydrates and the results obtained agree with experimental values.

A somewhat different method for calculations of phase transitions in the system methane–water was proposed.[58, 59] Calculations were carried out based on the model of intermolecular interactions using the Monte Carlo method. This is a general approach. The Monte Carlo method was used to determine the properties of the solid phase, while the properties of the fluid phases were calculated using the thermodynamic perturbation theory. According to calculations, such a simple molecular model allows one to describe the phase diagram of the system methane–water and to obtain qualitative agreement with the experiment. Monte Carlo simulation was also used to evaluate a number of approximations in the van der Waals–Platteeuw theory and some its extensions.

A simple thermodynamic model for estimation of the solubility of pure hydrocarbon hydrates (methane, ethane, propane) in pure water in equilibrium with gas hydrates was developed.[60–62] The results of calculations based on this model are in reasonable agreement with experimental data.

Yet another thermodynamic model[63] includes only two fitting parameters. It enables accurate calculations of the hydrate–water–vapour phase equilibria for gas hydrates containing one guest molecule at temperatures below 300 K. It was shown that calculations using this model give smaller deviations from experimental data compared to other known models. In addition, it was found that the solubility of guest molecules in water has little effect on the accuracy of calculations.

A mathematical model for evaluation of the effect of temperature on equilibria in the vapour–solid phase system was proposed.[64] Calculations using this model are simpler and more accurate than those based on the equation of state. Numerical calculations of the formation of gas hydrates in multicomponent mixtures including methane, ethane, propane, carbon dioxide and hydrogen sulfide were carried out.

Below we present a detailed consideration of the model of ideal gas hydrate. It allows the properties of gas hydrates to be determined rather accurately without fitting parameters.

5. Calculations of the Langmuir coefficients

The models considered above are based on calculations of the Langmuir coefficients [see Eqns (1) and (2)]. They can be determined using the results of a study[65] in which the spherical cell model was proposed. Having replaced the average radius of a cell formed by neighbouring molecules in the liquid by the average radius (R_i) of the cavity formed by water molecules, the authors of Ref. 65 derived the following equation

$$C_i = \frac{4\pi}{kT}\int_0^{R_i} \exp\left(-\frac{W(r)}{kT}\right) r^2 \mathrm{d}r, \tag{5}$$

where $W(r)$ is the radial potential function obtained using the potential of the interaction between gas molecules and surrounding water molecules and r is the distance from the centre of the cavity to the inserted gas molecule.

As shown above, the interaction between gas molecules within the hydrate cavities can be ignored. The energy of the gas–water interaction is usually determined by the Lennard-Jones potential; however, other potentials can also be used. For instance, it was proposed[66, 67] to use the spherical Kihara potential because it seems to provide a better description of the equilibrium of hydrates than other potentials. The Kihara potential has the form

$$F(x) = 4\varepsilon\left[\left(\frac{\sigma}{x-2a}\right)^{12} - \left(\frac{\sigma}{x-2a}\right)^{6}\right] \text{ at } x > 2a, \tag{6}$$

where $F(x)$ is the potential energy of the interaction between water and gas molecules separated by the distance x; ε is the depth of the potential well; σ is the distance between the molecular centres for which $F(x) = 0$; and a is the parameter that takes account of the length of the molecule. The spherically symmetric smoothed potential $\langle W(r)\rangle$ derived from the cell model is expressed through the parameters of the Kihara potential as follows:

$$\langle W(r)\rangle = 2Z\varepsilon\left[\frac{\sigma^{12}}{R^{11}r}\left(B^{10} + \frac{a}{R}B^{11}\right) - \frac{\sigma^6}{R^5 r}\left(B^4 + \frac{a}{R}B^5\right)\right], \tag{7}$$

where Z is the coordination number, R is the radius of the cavity,

$$B^n = \frac{1}{n}\left[\left(1 - \frac{r}{R} - \frac{a}{R}\right)^{-n} - \left(1 + \frac{r}{R} - \frac{a}{R}\right)^{-n}\right], \tag{8}$$

and n can be equal to 4, 5, 10 or 11.

Improvement[66–69] of the model for calculations of the Langmuir coefficients made it possible to describe experimental data more correctly.

The radius and coordination number for each cavity were determined.[66] This allows one to use the parameter $\langle W(r)\rangle$ for approximation of the potential of the interaction in the cavity for all distances where this potential, either negative or positive, is small in absolute value. Also, it is not necessary that the coordination number of the equivalent spherical cavity be equal to the actual coordination number of the cavity.

The results of dissociation pressure calculations for a number of substances carried out using this model are in good agreement with experimental data.[68, 69]

Thus, the system of equations (5), (7), (8) makes it possible to calculate the Langmuir coefficients necessary for the determination of conditions for the existence of gas hydrates using Eqns (1)–(3).

An algorithm and the results of calculations of gas hydrate parameters for separation and high purification of gases using the model of ideal solutions and the spherical cell model for the determination of the Langmuir coefficients were reported.[70] To verify the correctness of the results obtained, the Langmuir coefficients for argon, krypton and xenon hydrates were calculated using these methods

and then compared with the corresponding experimental data.[71] The results of calculations appeared to be in good agreement with the experimental data.

III. Separation of gaseous components during gas hydrate crystallization

If a hydrate-forming gas represents a mixture of gases M_1, $M_2, \ldots, M_i$, the formation of mixed hydrates is possible at corresponding pressures and temperatures. The composition of such systems change on decomposition. The simplest example of mixed hydrates is provided by double hydrates $M_1 + M_2$. Gaseous components are redistributed between the gas hydrate and gas mixture.[3] The gas hydrate (or gas mixture) is enriched (or depleted) with one or more components due to the differences in the chemical compositions of the equilibrium gas and solid (on anhydrous basis) phases.[70] This effect was experimentally established in the separation and concentration of noble gases[2] and components of natural gas.[7] The dissociation pressure of the mixed gas hydrate depends strongly on the composition and temperature of the gas mixture.[72,73] If the gas mixture contains a component with a lower dissociation pressure of its gas hydrate, this component is responsible for the decrease in the dissociation pressure of the mixed hydrate.

Recently, this property has found a practical application.[74–76] Mention was made[74] that clathrate hydrates are promising for storage and transportation of various gases. In particular, chlorinated hydrocarbons can be removed from water using the hydrate techniques with CO_2, N_2, CH_4 as hydrate-forming gases.[75] The stability boundaries of the hydrate $CO_2-N_2-H_2O$ in the presence (or in the absence) of tetrahydrofuran were determined by measuring phase equilibria.[76] Based on the results obtained, a process for CO_2 recovery from flue gases by hydrate separation of gas was developed; it appeared to be more efficient than the existing separation techniques. An apparatus for the hydrate process of helium recovery from natural gas was patented.[77] It was also proposed[9] to isolate hydrogen isotopes during separation of normal and heavy water by column gas hydrate crystallization. Gas hydrates can be used as selective stationary phases in chromatography.[78]

Gas hydrates are considered as a new class of impurities in high-purity substances.[3,30] This particularly concerns the formation of double or mixed gas hydrates. Here, the crystal framework of a gas hydrate can contain molecules of other gases that act as impurities.[79]

The results of theoretical and experimental studies on the separation of mixtures and purification of gases by the gas hydrate crystallization method were reported.[72,79–84] An algorithm was proposed for calculating the distribution coefficients of components of gas mixtures during the gas hydrate crystallization. It is constructed taking into account the known parameters of the interaction of gas hydrates and impurity molecules.

1. The distribution coefficients of gas mixture molecules in the cavities of mixed hydrates

In studies of mixed hydrates of noble gases and a gas-hydrate-forming gas (most often, sulfur dioxide), the fractionation coefficient is defined as follows[2]

$$K_f = \frac{d_p}{100 - d_p} \frac{100 - d_0}{d_0}, \tag{9}$$

where d_p and d_0 are respectively the fractions (in %) of the major component (sulfur dioxide) and the distributing substance (noble gas) in the gas hydrate form. The fractionation coefficient is determined from experimental data and this does not allow one to assess how the components are redistributed between the gas hydrate and gas mixture from calculations using parameters of the interaction of the gas hydrates and included molecules (impurities).

It was proposed[30,72] to characterize the distribution of molecules in cavities of a gas hydrate using the distribution coefficient which is calculated from the data on the fraction of filled cavities in the gas hydrate and on the composition of the gas mixture. The expression for this coefficient has the form:

$$K_i = \frac{Q_i P_s}{p_i \sum_i Q_i}, \tag{10}$$

where Q_i is the fraction of the hydrate cavities filled with the molecules M_i, P_s is the total pressure of the gas mixture, p_i is the partial pressure of the molecules M_i in the gas mixture, and ΣQ_i is the total fraction of the cavities filled with the molecules of the hydrate-forming gas.

The fraction of the type-j cavities filled with the type-i gas molecules is determined from the equation

$$Q_{ij} = \frac{C_{ij} f_i}{1 + \sum_i C_{ij} f_i}, \tag{11}$$

where C_{ij} are the Langmuir coefficients calculated using the spherical cell model for the type-i gas in the type-j cavity;

$$f_i = p_i \varphi_i$$

is the fugacity of the ith gas; p_i is the pressure of the ith gas; and φ_i is the fugacity coefficient.[71]

If n_j is the fraction of the type-j cavities in gas hydrate, one gets

$$Q_i = \sum_j n_j Q_{ij}. \tag{12}$$

To characterize the redistribution of components of the gas mixture during the formation of gas hydrates, the relative distribution coefficient was introduced[30,72]

$$K_{i1} = \frac{K_i}{K_1}, \tag{13}$$

where the component of the mixture with $i = 1$ is conditionally treated as the major component to be purified.

Substituting Eqn (10) into expression (13), one gets

$$K_{i1} = \frac{Q_i p_1}{Q_1 p_i}. \tag{14}$$

The value of the relative distribution coefficient suggests whether the gas hydrate is enriched ($K_{i1} > 1$) or depleted ($K_{i1} < 1$) in impurities from the substance to be purified. From the equations listed above it follows that the relative distribution coefficient depends strongly on the hydrate formation conditions and on the impurity concentration in the gas mixture.

The effect of the hydrate formation conditions and the composition of the gas mixture on this coefficient was studied.[72,80–82] It was shown that the K_{i1} value depends strongly on the component ratio in the gas mixture and can appreciably differ from unity for identical conditions. Therefore, depletion or enrichment of the major component in impurities containing in hydrate is possible even in the stage of hydrate formation. Having separated gas hydrates from the gas mixture, one can additionally purify the major gaseous substance or air–gas mixtures.

The effect of the hydrate formation conditions and the impurity concentration in the gas mixture on the magnitude of the relative distribution coefficients of some impurities in the formation of gas hydrates in sulfur hexafluoride was studied.[81] The concentration ranges of the main hydrate-forming impurities (c_i) in sulfur hexafluoride are listed below.

Impurity	N_2	CO_2	SO_2	O_2
c_i (vol.%)	0.02–0.2	0.015–0.2	0.001–0.025	0.005–0.05

Consider a three-component gas mixture SF_6-H_2O-impurity.[81] The results of calculations of the dependences of the distribution coefficient on the impurity concentration, temperature and pressure are shown in Figs 1–3. Since in all cases the partial pressure of water is much lower than the partial pressure of impurity in the gas mixture, the concentration of the mixture H_2O+impurity can be considered equal to the impurity concentration. The error in calculations of the distribution coefficients due to inexact values of the Kihara potential parameters is at most 10% for sulfur dioxide and carbon dioxide and 15% for oxygen and nitrogen. This error was determined by varying the parameters of the potential, *i.e.*, by calculating the changes in the distribution coefficient determined from Eqns (5), (6), (12) and (13) using the maximum and minimum values of the parameters of the Kihara potential.[81]

For more convenient analysis of the dependences thus obtained, Eqn (11) was transformed[81] taking into account the fact that the following relations between the Langmuir

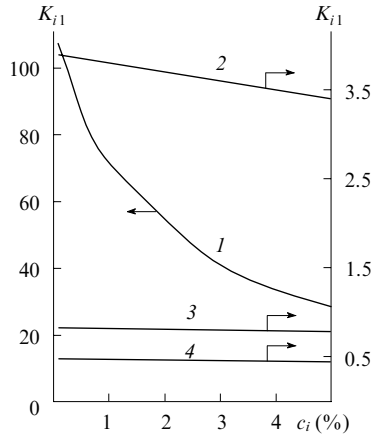


Figure 1. Concentration dependences of the relative distribution coefficients of impurities.[81]
Gas mixture composition: 99.5% SF_6 + 0.5% (H_2O + impurity); P = 400 kPa; T = 273 K; impurity: SO_2 (*1*), CO_2 (*2*), O_2 (*3*), N_2 (*4*).

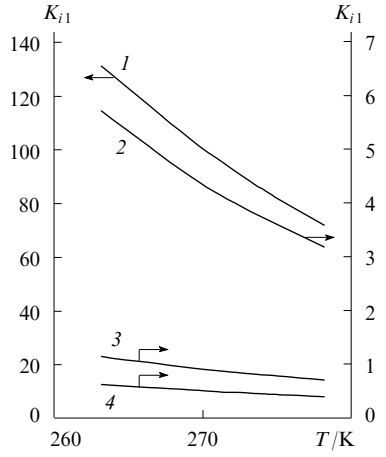


Figure 2. Temperature dependences of the relative distribution coefficients of impurities.[81]
Gas mixture composition: 99.5% SF_6 + 0.5% (H_2O + impurity); P = 1000 kPa; (*1–4*) see Fig. 1.

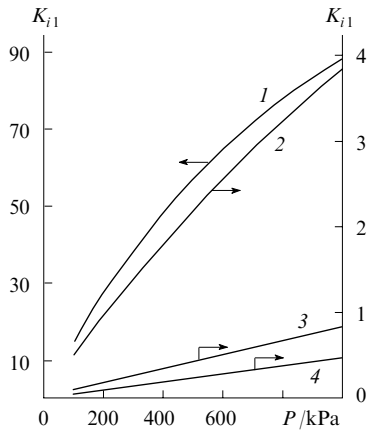


Figure 3. Dependences of the relative distribution coefficients of impurities on the pressure in the system.[81]
Gas mixture composition: 99.5% SF_6 + 0.5% (H_2O + impurity); T = 273 K; (*1–4*) see Fig. 1.

coefficients hold for the temperature range in question and for all studied components of the gas mixture:

$$C_{i1} \ll 1;\ C_{11} \ll C_{i1};\ C_{i1} \ll C_{i2};\ C_{i2} \ll C_{12}. \qquad (15)$$

Here, the first subscript '1' denotes the major component, the subscript i denotes the impurity and the second subscripts '1' and '2' refer to the small and large cavity, respectively. Taking into account this condition and having transformed Eqns (11), (12) and (14), the equation for the determination of the relative distribution coefficient of the impurities takes the form

$$K_{21} = \frac{2\varphi_2 p_1 C_{12}}{1 + C_{12}\varphi_2 p_2}, \qquad (16)$$

where φ_2 is the fugacity coefficient of the impurity.

From Eqn (16) it follows that the relative distribution coefficient is determined by the Langmuir coefficients of the

impurity for small cavities, by the partial pressures of the major component and impurity and by the fugacity coefficient of the impurity. This is due to the fact that the sulfur hexafluoride molecules occupy almost all large cavities in the gas hydrate, as follows from relations (15), and the distribution coefficient is only affected by the fraction of small cavities filled with the impurity molecules.

Impurities in SF_6 can be divided into three groups. The first group includes O_2 and N_2 characterized by $K_{21} \ll 1$. Small relative distribution coefficients of these impurities are due to a very low fraction of hydrate cavities filled with the impurity molecules owing to the small Langmuir coefficients for small cavities ($C_{12} \sim 10^{-4}$ kPa^{-1} for nitrogen and oxygen). In this case, $C_{12}\varphi_2 p_2 \ll 1$ and Eqn (16) takes the form

$$K_{21} = 2\varphi_2 p_1 C_{12}. \tag{17}$$

From Eqn (17) it follows that for these impurities the changes in the relative distribution coefficients with the changes in the impurity concentration and the total pressure of the gas mixture are solely determined by the fugacity coefficient of the impurity and by the partial pressure of the major component. As the impurity concentration increases, p_1 decreases; this leads to a decrease in the relative distribution coefficient (see Fig. 1). An increase in the total pressure of the gas mixture causes the partial pressure of sulfur hexafluoride to increase and the relative distribution coefficient monotonically increases (see Fig. 3). In both cases, the fugacity coefficients of the impurities in question remain almost unchanged.

From Eqn (17) it follows that the temperature dependence of the relative distribution coefficient is mainly determined by the temperature dependence of the Langmuir coefficient of the impurity for the small cavity. As temperature increases, the Langmuir coefficient decreases and one deals with redistribution of the gases in the hydrate cavities. The fraction of the cavities filled with impurities decreases; therefore, the relative distribution coefficient also decreases (see Fig. 2).

The second group of impurities includes CO_2 whose relative distribution coefficient is close to unity due to the much higher value of the Langmuir coefficient for small cavity ($C_{12} \approx 10^{-3}$ kPa^{-1}). If the concentration of carbon dioxide in a gas mixture is low, one has $C_{12}\varphi_2 p_2 \ll 1$ and the dependence of the relative distribution coefficient on the parameters of the process is again analyzed using Eqn (17). As for the first group of impurities, in this case the dependence of the relative distribution coefficient on the impurity concentration and on the pressure of the gas mixture is determined by the fugacity coefficient of carbon dioxide and by the partial pressure of sulfur hexafluoride (see Figs 1 and 3). At low pressures, the distribution coefficient of carbon dioxide is less than unity. As the pressure of the gas mixture increases, the distribution coefficient of carbon dioxide increases and becomes larger than unity. Such a behaviour of this parameter is due to the fact that the fraction of the large cavities filled with the sulfur hexafluoride molecules remains almost unchanged with an increase in the pressure of the gas mixture, whereas the fraction of the small cavities occupied by the carbon dioxide molecules increases in proportion to an increase in its partial pressure. From Eqn (17) it follows that $K_{21} = 1$ at $p_1 = 1/2\,\varphi_2 C_{12}$.

As for the first group of impurities, the temperature dependence of the relative distribution coefficient of carbon dioxide (see Fig. 2) is determined by the temperature dependence of the Langmuir coefficient in Eqn (17).

The third group of impurities includes sulfur dioxide characterized by the relative distribution coefficient greater than unity. The concentration dependence of the relative distribution coefficient of this impurity was analyzed[81] using Eqn (16). As the sulfur dioxide concentration in the gas mixture at constant pressure increases, the partial pressure of sulfur dioxide increases. The partial pressure of sulfur hexafluoride decreases, which leads to a decrease in the relative distribution coefficient (see Fig. 1). As the pressure of the gas mixture increases, the partial pressure of sulfur hexafluoride increases and, therefore, the distribution coefficient also increases (see Fig. 3).

As in the preceding cases, a decrease in the relative distribution coefficient with an increase in temperature (see Fig. 2) is mainly due to a decrease in the Langmuir coefficient in Eqn (16).

Consider a four-component mixture $SF_6 - H_2O -$ impurity 1 – impurity 2.[81] The impurity concentrations were chosen based on their actual concentrations in raw gas.

For the four-component system, Eqn (16) can be transformed to

$$K_{21} = \frac{2\varphi_2 p_1 C_{12}}{1 + C_{12} f_2 + C_{13} f_3}, \tag{18}$$

where the subscripts '1', '2', 3' refer to the major component, first impurity and second impurity, respectively.

From Eqn (18) it is seen that, if the gas mixture contains only components with small Langmuir coefficients (impurities from the first and second groups), for the products one has $C_{12} f_2 \ll 1$ and $C_{13} f_3 \ll 1$ and they can be neglected; then Eqn (18) is transformed to Eqn (17). In this case, other impurities present in the mixture do not influence the distribution coefficient. If sulfur dioxide acts as impurity, Eqn (18) takes the form:

$$K_{21} = \frac{2\varphi_2 p_1 C_{12}}{1 + C_{13} f_3}. \tag{19}$$

Here, the subscript '3' refers to sulfur dioxide. Therefore, if the mixture contains sulfur dioxide, its effect should be taken into account in the determination of the distribution coefficients of other impurities. For instance, the change in the distribution coefficient of CO_2 is only affected by the sulfur dioxide molecules, *viz.*, the addition of sulfur dioxide to the gas mixture causes the relative distribution coefficient of CO_2 to decrease, as follows from Eqn (19). As the temperature increases and the pressure decreases, this effect becomes less pronounced. The distribution coefficients of other impurities change analogously.

Therefore, practical calculations of the separation of gas mixture components at negative temperatures and high pressures should take into account the presence of impurities with large Langmuir coefficients.

Thus, it was shown[81] that, during purification of sulfur hexafluoride, gas hydrates will be enriched in sulfur dioxide ($K_{21} > 1$) and depleted in nitrogen and oxygen ($K_{21} < 1$). Depending on the pressure, the distribution coefficient of carbon dioxide can be smaller (at low pressures) or greater

than unity. The distribution coefficients of other impurities under study significantly differ from unity.

The results of calculations of the relative distribution coefficients for an air mixture containing the following impurities: sulfur and carbon dioxides, nitrogen(I) oxide, Freon-12 and chloroform were reported.[3, 80] They included the concentrations of these impurities in the gas hydrate calculated [80] as follows. Having known the fraction of the cavities filled with the gas mixture molecules and taking into account the fact that the structure I (structure II) hydrate is characterized by 5.75 (5.67) water molecules per cavity,[3] the mole fraction of gas relative to water can be determined from the equations

$$c_i = \frac{Q_i}{5.75} \text{ for structure I,} \qquad (20)$$

$$c_i = \frac{Q_i}{5.65} \text{ for structure II.}$$

For instance, at 263 K, hydrates will mainly contain sulfur dioxide and chloroform as impurities.

2. Experimental determination of the distribution coefficients in the systems gas – gas hydrate

If no initial data for calculations are available, the distribution coefficient can be determined from the experimental data on the equilibrium in the systems gas – gas hydrate. To this end, the gas phase is separated in the equilibrium state from the solid phase and the concentrations of the hydrate-forming components are determined for each phase.[7] This experiment is difficult from the standpoint of phase separation. The phase compositions were also calculated [7] from the equilibrium balance taking into account the changes in the pressure and volume of the gas phase in the formation of gas hydrates. However, this technique can be used if the Langmuir coefficients of the substances under study are known.

A method for experimental determination of the distribution coefficients of the gas mixture components under the gas hydrate crystallization conditions was proposed.[83, 84] The technique uses simple laboratory equipment and does not require knowledge of the physicochemical properties of the gas hydrates under study, labour-consuming isolation of the solid phase or determination of the composition of the gas phase in the gas hydrates.

The separation coefficient (α) for a binary gas mixture containing a major component and an impurity is given by the known expression

$$\alpha = \left(\frac{c_h}{1-c_h}\right)\left(\frac{c_g}{1-c_g}\right)^{-1}, \qquad (21)$$

where c_h is the impurity concentration in the gas hydrate; c_g is the impurity concentration in the gas phase that is in equilibrium with the gas in the hydrate. In the case of the gas hydrate crystallization one has

$$c_h = \frac{Q_i}{Q},$$

$$c_g = \frac{p_i}{P}$$

and Eqn (21) is transformed to the equation for the relative distribution coefficient (14).

Expression (21) allows one to determine the separation coefficient from the experimental data on the equilibrium between the gas and gas hydrate phases. The equilibrium parameters of gas hydrates were studied by the static method under isothermal conditions. In this case, the impurity concentration in the gas phase can be determined analytically. To prevent changes in the composition of the equilibrium phases, small amounts of the gas phase were analyzed. The equilibrium impurity concentration in the gas hydrate was determined [83] as described below using the mass balance equation for the gas hydrate crystallization under static conditions. A mixture of gases A + B (a total of N_0 moles) fills some volume at the initial pressure P_0 and constant temperature T. The pressure P_0 is higher than the dissociation pressure of the gas hydrates formed by the individual components A or B at the specified temperature T. In the course of gas hydrate crystallization, a fraction of the gas mixture (N_h moles) goes to the gas hydrate and the gas phase now contains N_g moles of the gas. Therefore, the mass balance for gas hydrate crystallization with respect to the gas phase can be written as follows:

$$N_0 = N_h + N_g; \qquad (22)$$

for the impurity component of the gas mixture one has

$$n_0 = n_h + n_g, \qquad (23)$$

where n_0, n_g are the initial and final amounts of the impurity in the gas mixture; and n_h is the amount of impurity in the gas hydrate.

If the initial impurity concentration in the gas mixture is c_0, the amount of impurity in the gas phase at the initial instant is:

$$n_0 = N_0 c_0. \qquad (24)$$

The amount of gas consumed for the gas hydrate formation can be determined if we know the fraction of the gas (θ) that crystallized as gas hydrate,

$$N_h = N_0\theta. \qquad (25)$$

Then, the amount of impurity in the gas hydrate is

$$n_h = N_h c_h = N_0 c_h \theta. \qquad (26)$$

The total amount of components remaining in the gas phase is

$$N_g = N_0 - N_h = N_0(1-\theta). \qquad (27)$$

Taking into account expressions (25) and (27), the amount of impurity in the gas phase is

$$n_g = N_g c_g = c_g N_0(1-\theta). \qquad (28)$$

Thus, taking into account expressions (24), (26) and (28), the mass balance equation (23) for the impurity takes the form

$$N_0 c_0 = N_0 c_h \theta + N_0 c_g(1-\theta). \qquad (29)$$

The impurity concentration in the gas hydrate is given by

$$c_h = \frac{c_0 - c_g(1-\theta)}{\theta}. \quad (30)$$

Substituting expression (30) into Eqn (21), one gets

$$\alpha = \left(\frac{1-c_g}{c_g}\right)\left(\frac{\theta}{c_0-(1-\theta)c_g} - 1\right)^{-1}. \quad (31)$$

Therefore, knowledge of the impurity concentration in the initial mixture and in the gas phase that is in equilibrium with the gas hydrate, as well as the fraction of the gas that crystallized in the form of gas hydrate allows one to determine the separation coefficient in the system gas–gas hydrate.

This method of determination of the distribution coefficient was tested on the system $SF_6-CF_2Cl_2$. The concentration of CF_2Cl_2 in the gas mixture was 13.6 vol.%. This system was chosen because gas hydrates formed by its components are well studied and characterized by low dissociation pressures, *viz*., 86.5 and 34.7 kPa for the SF_6 and CF_2Cl_2 hydrates, respectively, at 0 °C.[7] To study the effect of experimental conditions on the accuracy of determination of the separation coefficient, hydrate formation was performed[83] at 272, 273 and 275 K in excess amount of water (35, 100 and 150 ml). In addition, some experiments were carried out using a stirrer during the formation and growth of gas hydrates.

The design of the experimental apparatus is shown in Fig. 4. The key unit is a 330 ml gas hydrate cell. A horizontal cylindrical cell is made of stainless steel and has a viewing window and external cooling jacket. The design includes the system of fine control of the gas inflow rate and the sample outflow rate, a thermostat, a vacuum system and a mechanism for reneval of the interface (a shaker or a stirrer). The feeding and sampling lines were combined to provide a minimum sample volume. The thermostat maintains the temperature using a 'Proterm-100' controller with an accuracy of 0.1 °C. The apparatus allows one to study the hydrate formation at pressures up to 1000 kPa with an accuracy of 2 kPa.

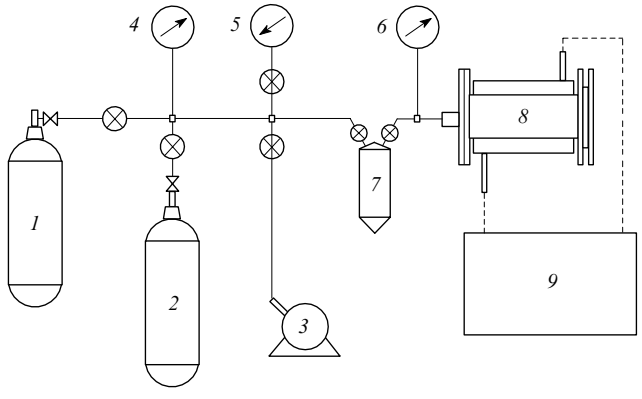


Figure 4. Design of experimental apparatus.[83]
Helium container (*1*), gas mixture bottle (*2*), vacuum pump (*3*), standard pressure gauge (*4*), vacuum gauge (*5*), pressure vacuum gauge (*6*), sampling cylinder (*7*), crystallizer (*8*) and thermostat (*9*).

Experimental determination of the distribution coefficients was done as follows.[83] The cell was filled with a specified amount of water and gas mixture and the desired temperature was set. Preliminary experiments involved the formation of a particular amount of gas hydrate. To this end, the gas mixture in the cell at the initial instant of time was kept at a high excess pressure P_0. As mixed gas hydrates formed from the gas mixture, the pressure in the system slowly decreased to P_e. As a constant pressure was reached, the equilibrium was attained by long-term storage of the gas hydrates under static conditions.[2,7]

Different authors report different storage times, from two hours[7] to a few days.[24] Therefore, preliminary experiments with this system were carried out to determine the minimum time interval necessary to attain the equilibrium state.[83] As a result, the dependence of the distribution coefficient of CF_2Cl_2 between the gas and solid phases on the storage time of gas hydrates was obtained (see Fig. 5). The distribution coefficient was calculated using Eqn (31). As can be seen, gas hydrates should be kept for at least 120 min under static conditions to attain equilibrium. This is indicated by independence of the distribution coefficient value on time (the curve reaches a plateau at $t > 120$ min).

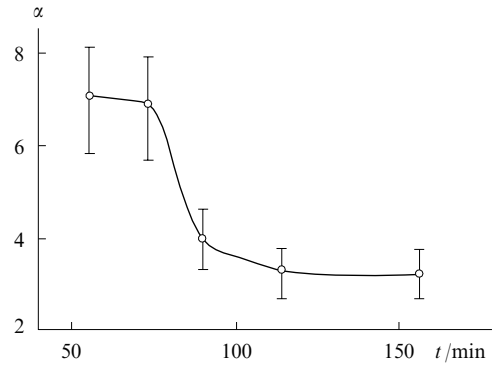


Figure 5. Separation coefficient plotted *vs*. time of storage of gas hydrates under static conditions: $T = 273$ K, $P_0 = 2.5$ atm, $K_{i1} = 2.63$ (SF_6 as major component, CF_2Cl_2 as impurity).[83]

After completion of the experiments, a small amount of gas mixture was sampled. The concentration of CF_2Cl_2 in the sample was determined following a known procedure.[85] The error in GC analysis was at most 5%.

The separation coefficients for different experimental conditions were calculated using expression (31). The fraction of gas that crystallized as gas hydrate was determined as follows:

$$\theta = \frac{P_0 - P_e}{P_e}, \quad (32)$$

where P_0 and P_e are the initial and final pressure in the system, respectively. The error in the determination of the separation coefficient using relation (31) was 16%.

The results obtained in these experiments are in good agreement with those reported in a theoretical study.[81]

To verify the experimental data, the relative distribution coefficient was calculated from expression (14) based on the theory of ideal solid clathrate using a known procedure.[3,80] The Langmuir coefficients were calculated using the Kihara

potential. The parameters of the intermolecular interaction potential for the substances under study were as follows:

for SF_6

$\frac{\varepsilon}{k}$ = 312 K, σ = 3.77 Å, a = 0.4 Å;

for CF_2Cl_2

$\frac{\varepsilon}{k}$ = 419.1K, σ = 3.70 Å, a = 0.36 Å.

They were obtained from the dissociation pressure values for the corresponding gas hydrates using a procedure described elsewhere.[86] The results of calculations of the relative distribution coefficients are listed in Tables 1 and 2. The coefficients α and K_{i1} differ by 13%, which lies within the limits of the error of the technique employed. The accuracy in determination of the separation coefficient from experimental data is independent of the amount of water in the system and of the temperature at which crystallization of the gas hydrate is carried out. The use of a stirrer also has no effect on the accuracy of the results obtained; it only favours the attainment of equilibrium in the system.

Table 1. Results of determination of the coefficients α and K_{i1} at different amounts of water in the system (P_0 = 250 kPa, T = 273 K, c_0 = 13.6 vol.%).[83]

Water volume /ml	c_g (vol.%)	c_h (vol.%)	P_e /atm	θ	α (see [a])
35	7.1	15.8	0.79	0.69	2.48
100 [b]	6.5	16.3	0.83	0.67	2.81
100	6.5	16.4	0.84	0.66	2.86
150	6.6	16.3	0.83	0.67	2.78

Note. In all cases, calculations using expression (14) showed that K_{i1} = 2.63. [a] Calculated using expression (31). [b] Experiments were carried out under mixing.

Table 2. Results of determination of the coefficients α and K_{i1} at different temperatures (P_0 = 250 kPa, c_0 = 13.6 vol.%).[83]

T/K	c_g (vol.%)	c_h (vol.%)	P_e /atm	θ	α (see [a])	K_{i1} (see [a])
272	6.0	16.0	0.73	0.71	2.96	2.62
273	7.1	15.8	0.79	0.69	2.48	2.63
275	8.2	17.3	1.16	0.54	2.34	2.66

[a] Calculated using expression (31). [b] Calculated using expression (14).

Thus, the method [86] allows one to determine the distribution coefficient in the system gas – gas hydrate with a reasonable accuracy.

3. Determination of parameters of intermolecular interaction in gas hydrate

Theoretical calculations of hydrate formation conditions require knowledge of the parameters of the potential of intermolecular interaction between gas molecules in the cavity of a gas hydrate (guest molecules) and water molecules that form the crystal framework (host molecules).[3] Parameters of the potential of the host – guest interaction can be determined using the Lorentz – Berthelot mixing rule and the corresponding parameters of individual substances (guest – guest interaction). However, for many hydrate-forming gases these data are unknown or contradictory. In addition, if the parameters of the potential of intermolecular interaction were determined from the viscosity data or from the second virial coefficient in the equilibrium state represented by a polynomial in powers of the reciprocal volume, they should be corrected taking into account the properties of the corresponding gas hydrates.[86] The numerical values are refined by comparing the results of calculations of the dissociation pressure and the compositions of the hydrate and gas phases with experimental data.

A scheme for calculations of the Kihara potential parameters for methane and ethane from experimental data on hydrate formation was proposed.[87] The scheme uses the values of the parameters as fitting ones. Calculations of the phase equilibrium using the Kihara potential parameters thus obtained predict a transition from structure I to structure II in mixed hydrates, which agrees with experimental data.

A mathematical method [57] involving analytical determination of the potential of the host – guest' interaction in clathrate hydrates allows one to calculate parameters of the interaction potential for hydrates with the known Langmuir coefficients.

It was also proposed [88] to determine parameters of guest – guest intermolecular interaction by regression analysis using experimental data on the distribution coefficient of the gas under study mixed with a well-studied component during gas hydrate crystallization. The theory of ideal clathrate and experimental data are used to calculate the parameters of the host – guest intermolecular interaction. They are suitable for calculating the guest – guest interaction parameters. Subsequently, the distribution coefficients are determined for different conditions of gas hydrate crystallization. These coefficients were shown to be in reasonable agreement with experimental data.

The relative distribution coefficient is calculated from Eqns (5), (11) and (14). To obtain the radial function in Eqn (5), one can use the interaction potentials similar to the Lennard-Jones or Kihara potentials.

The potential function $\langle W_i(r)\rangle$ can be expressed through the parameters of the Lennard-Jones 12 – 6 potential:

$$\langle W_i(r)\rangle = 2Z\varepsilon\left(\frac{\sigma^{12}\delta^{10}}{R^{11}r} - \frac{\sigma^6\delta^4}{R^5}\right), \tag{33}$$

where Z is the coordination number, R is the radius cavity;

$$\delta^N = \frac{1}{N}\left[\left(1-\frac{r}{R}\right)^{-N} - \left(1+\frac{r}{R}\right)^{-N}\right], \tag{34}$$

and N can be equal to 10 or 4.

The results of dissociation pressure calculations for gas hydrates using the 12 – 6 Lennard-Jones potential agree well with the experimental data for molecules of polyatomic gases and small spherical molecules (*e.g.*, CH_4). For rod-like molecules (*e.g.*, N_2, O_2, N_2O, CO_2, *etc.*), the best results were obtained with the quasi-spherical Kihara potential (6) which takes into account the effect of the molecular extension, shape and symmetry on the interaction energy.

The radial function $\langle W_i(r)\rangle$ expressed through the Kihara potential parameters is specified by Eqns (7) and (8).

The parameters ε and σ of the interaction between the molecules of the type-i component of the gas mixture and water molecules appeared in expressions (6) and (33) are determined using the Lorentz – Berthelot rule:

$$\varepsilon = \sqrt{\varepsilon_w \varepsilon_{gi}}, \qquad (35)$$

$$\sigma = \frac{\sigma_w + \sigma_{gi}}{2},$$

where $\sigma_w = 3.564$ Å and $\varepsilon_w/k = 102.1$ K are the parameters of the intermolecular interaction for water molecules [69] and σ_{gi}, ε_{gi} are the parameters of the intermolecular interaction for pure type-i component of the gas mixture (guest – guest interaction).

Having specified combinations of the parameters σ_{gi} and ε_{gi} of the interaction potential of the substance under study in Eqns (35) and having solved the chain of equations (7), (8) or (33), (34), (5), (11), (14), one can choose such parameter values that provide the relative distribution coefficient equal to the known values for different conditions. Thus, having experimentally determined the distribution coefficient of a substance under study mixed with a well-studied component, one can find the parameters of the potential of intermolecular interaction for the pure substance.

The parameters σ_{gi} and ε_{gi} of the interaction potential for the system $SF_6 - CCl_2F_2$ were calculated.[88] Both molecules have a spherical shape, dichlorodifluoromethane has a small dipole moment (0.55 D) while the sulfur hexafluoride molecule is nonpolar; therefore, the system in question can with reasonable accuracy be described by the Lennard-Jones potential. This system was chosen taking into account the fact that gas hydrates formed by SF_6 and CF_2Cl_2 are well studied and vast information on their dissociation pressures and distribution coefficients is available.

First, we will consider the case where the role of the substance under study is played by the major component of the mixture, *viz*., sulfur hexafluoride. The necessary values of the parameters, σ_{g1} and ε_{g1}, of the Lennard-Jones potential were preliminarily obtained by regression analysis from the hydrate composition and dissociation pressure data following the known procedure:[86]

for CF_2Cl_2

$$\frac{\varepsilon_{g1}}{k} = 335.5 \text{ K}, \ \sigma_{g1} = 4.06 \text{ Å};$$

for SF_6

$$\frac{\varepsilon_{g1}}{k} = 261.0 \text{ K}, \ \sigma_{g1} = 4.28 \text{ Å}.$$

The published [89] experimental values of the equilibrium distribution coefficient for this system differ by 10% from the calculated value. The temperature was measured with an accuracy of 0.1 K. The distribution coefficients of the components of the gas mixture with an equilibrium CF_2Cl_2 concentration of 6 vol.% were calculated using expression (14) and the Lennard-Jones potential parameters listed above. The pressure of the gas mixture was assumed to be equal to the dissociation pressure of the gas hydrate $SF_6 - CF_2Cl_2$ (72.2, 117.5 and 198.5 kPa at 273.1, 275.1 and 277.1 K, respectively). The experimental and calculated values of the equilibrium distribution coefficient are listed in Table 3.

Table 3. Equilibrium (K), experimental (K') and calculated (K'') values of the distribution coefficient at different temperatures.[88]

T/K	K	K'	K''	Deviation K'' from K' (%)
273.1	2.24	2.41	2.42	0.4
275.1	2.32	2.53	2.50	1.2
277.1	2.45	2.60	2.62	0.8

Solution of the system of equations (5), (11), (14), (34) with respect to σ_{g1} and ε_{g1} for SF_6 allowed one to determine the parameters corresponding to the minimum deviations of the calculated values of the distribution coefficient from experimental ones for the entire temperature range studied (see Table 3). The parameters are $\varepsilon_{g1}/k = 258.34$ K and $\sigma_{g1} = 4.28$ Å; the corresponding calculated distribution coefficients are listed in Table 3. As can be seen, the distribution coefficients calculated using these data agree with experimental values.

The applicability of the σ_{g1} and ε_{g1} thus obtained to calculations of the conditions for gas hydrate formation was assessed by comparing the calculated and experimental values of the dissociation pressures of the gas hydrates. The dissociation pressures were determined within the framework of the theory of ideal solid clathrate using the Lennard-Jones potential parameters determined from the distribution coefficient data. The results obtained are listed in Table 4. As can be seen, the calculated dissociation pressure values are in reasonable agreement with the published data.

Table 4. Dissociation pressure of SF_6 gas hydrate.[88]

T/K	P'/kPa	P''/kPa	Deviation P'' from P' (%)
273.15	86.5	84.5	2.3
275.15	136	138.5	1.8
277.15	200	236.5	18.3

Note. Notations are as follows: P' denotes published data, P'' denotes the results of calculations.

Similar results were also obtained for the second case where the role of the substance under study is played by the minor component of the mixture, *viz*., CF_2Cl_2.[88] Therefore, both the major component and impurity can be studied experimentally.

The Lennard-Jones potential parameters for individual SF_6 and CF_2Cl_2 forming gas hydrates with the cubic structure II are in good agreement with the results of other studies [90–92] in which the dependence of the structure of clathrate hydrates on the parameters of the host – guest (ε/k, σ) and guest – guest (ε_{gi}/k, σ_{gi}) interaction potential was established.

Thus, experimental data on the distribution coefficients of the components of the gas mixture in the case of gas hydrate crystallization can be used for the determination of the intermolecular interaction parameters by regression analysis.

4. Gas hydrate crystallization at constant pressure and directed crystallization

Studies [85, 93–98] concern the applicability of the gas hydrate crystallization method to high purification of substances in the dynamic regime (formation of gas hydrates provided slow crystallization of the major component). In this case, one deals with precipitation of large crystals in which the concentration of impurity (substance to be distributed) changes from the centre to periphery. Each layer of the growing crystal is in equilibrium with the gas phase.

The efficiency of this technique is characterized by the separation coefficient [99]

$$\alpha = \frac{y}{1-y}\left(\frac{x}{1-x}\right)^{-1}, \tag{36}$$

where y is the impurity concentration in the gas mixture containing in the hydrate; and x is the impurity concentration in the gas mixture that is in equilibrium with the gas mixture in the hydrate.

The concentration of molecules of the type-i gas in the gas mixture containing in the gas hydrate is given by

$$y_i = \frac{Q_i}{Q},$$

where $Q_i = \sum n_j Q_{ji}$ is the fraction of the gas hydrate cavities filled with the type-i gas molecules; n_j is the fraction of the type-j gas hydrate cavities; Q_{ji} is the fraction of the type-j cavities filled with the type-i gas molecules; and $Q = \sum Q_i$ is the total fraction of the filled gas hydrate cavities.

The concentration of the type-i molecules in the gas mixture existing in equilibrium with the gas mixture in the hydrate is given by

$$x_i = \frac{p_i}{P_0},$$

where p_i is the partial pressure of the type-i gas and P_0 is the total pressure of the gas mixture.

Taking into account this expression, the relation for the separation coefficient has the form

$$\alpha = \frac{Q_i}{Q-Q_i}\left(\frac{p_i}{P_0-p_i}\right)^{-1}. \tag{37}$$

After rearrangements, expression (36) takes the form of the equation for the relative distribution coefficient (14).

Thus, in practical calculations of the separation of mixtures by the gas hydrate crystallization method the separation coefficient α can be determined by Eqn (14).

Two experimental regimes of gas hydrate crystallization, namely, an isobaric process and an analogue of directed crystallization have been considered.[85, 93, 97]

The former case is schematically shown in Fig. 6. A mixture of gases M_1 and M_2 (N_0 moles) fills a certain volume and is characterized by the pressure P_s which is higher than the dissociation pressure at the given temperature. At the water vapour pressure p_w (assuming p_w = const) equal to the saturated vapour pressure, stable formation of gas hydrates occurs. During the time interval dt, $m dN'$ moles of water (m is the number water molecules per gas molecule in the structure of gas hydrate) are crystallized as gas hydrates. The pressure of the gas mixture and the water vapour pressure are maintained constant due to the feeding of a mixture with the initial concentrations of the components and the necessary amount of water into the volume. A fraction of the gas mixture crystallizes as a hydrate and the remaining gas mixture is sampled in the form of purified product upon completion of the process.[85]

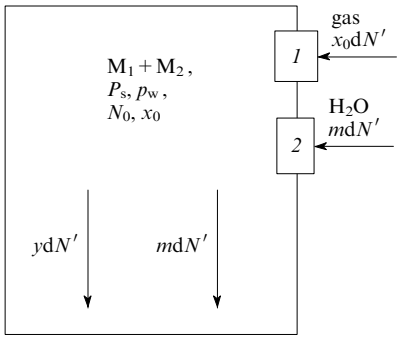


Figure 6. Separation of gas mixtures by the gas hydrate crystallization method under isobaric conditions: a schematic.
Gas and water vapour inlet systems (*1*, *2*); for the parameters of the process, see text.

The impurity concentration in the gas was taken to be the same in the entire volume.

The mass balance equation for the impurity has the form

$$d(N_0 x) = y\, dN' + x_0\, dN', \tag{38}$$

where N_0 (in moles) is the initial amount of the gas mixture in the volume considered; x_0 (in mole fractions) is the initial impurity concentration in the gas mixture; N' (in moles) is the amount of the gas mixture crystallized as gas hydrate.

Taking into account expression (36), the mass balance equation (38) takes the form

$$N_0\, dx = \frac{\alpha x}{1+(\alpha-1)x} dN' + x_0\, dN'. \tag{39}$$

A solution of this equation by the method of separation of variables with the initial condition $x = x_0$ at $N' = 0$ gave the dependence of the impurity concentration in the gas phase on the fraction of gas sampled from the gas hydrates, *i.e.*, on the fraction of the crystallized substance,

$$\frac{N'}{N_0} = -\frac{\alpha}{A^2}\ln\left[\frac{Ax - x_0}{x_0(A-1)}\right] + \frac{\alpha-1}{A}(x_0 - x), \tag{40}$$

where

$$A = \alpha - (\alpha-1)x_0.$$

If the fraction of the crystallized substance is

$$\theta = \frac{N'}{N'+N_0} = \frac{N'/N_0}{1+N'/N_0}, \tag{41}$$

by simultaneous solution of Eqns (40) and (41) one can determine the impurity concentration in the volume and the separation factor $F = x_0/x$ for a given fraction of the crystallized substance (Fig. 7). This requires that $M = mN'$ moles of water be fed into the volume [$m = 5.75/Q$ for structure I and $m = 5.67/Q$ for structure II (Ref. 3); m is the

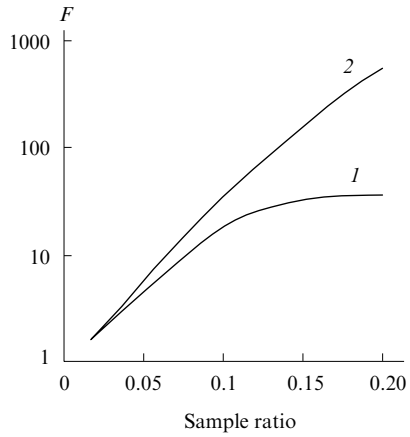


Figure 7. Plots of the separation factor of the mixture SF_6-SO_2 *vs.* sample ratio for the first (*1*) and second (*2*) regimes of gas hydrate crystallization.[85]
Impurity concentration is 1 mol.%, P_0 = 300 kPa, T = 273 K.

number water molecules per gas molecule in the structure of gas hydrate]. In addition, from Eqn (40) it follows that the limiting attainable impurity concentration in the volume corresponding to the maximum separation factor $F = A$, is x_0/A.

In the second case (directed gas hydrate crystallization), the pressure of the gas mixture in the volume continuously decreases due to the formation of gas hydrates, no gas mixture is additionally supplied and the purified product is sampled as the process is completed.[85,93,97] The impurity concentration in the gas is the same in the entire volume; at each instant, it is related to the impurity concentration in the gas mixture containing in the hydrate and described by Eqn (36). This regime of the process is analogous to the method of directed crystallization from melt.

The mass balance equation for this case has the form

$$\mathrm{d}\left(N''x\right) = y\,\mathrm{d}N'', \tag{42}$$

where N'' (in moles) is the amount of the gas mixture in the volume for the second regime of gas hydrate crystallization.

Taking into account expression (36), the mass balance equation takes the form

$$N''\mathrm{d}x = \frac{\alpha x}{1+(\alpha-1)x}\mathrm{d}N''\,. \tag{43}$$

A solution of this equation by the method of separation of variables with the initial condition $x = x_0$ at $N'' = 0$ gave the dependence of the impurity concentration in the gas phase on the fraction of the crystallized substance

$$\left(\frac{N''}{N_0}\right)^{\alpha-1} = \frac{x}{x_0}\left(\frac{1-x_0}{1-x}\right)^{\alpha}. \tag{44}$$

The fraction of crystallized substance is given by

$$\frac{N_0-N''}{N_0} = 1-\frac{N''}{N_0}\,. \tag{45}$$

Simultaneous solution of Eqns (44) and (45) makes it possible to determine the impurity concentration in the volume for a given fraction of the crystallized substance (see Fig. 7).

Experimental verification of the proposed mathematical models for calculations of the separation factor was carried out for the two designs of gas hydrate crystallization taking the system sulfur hexafluoride – Freon-12 impurity (separation coefficient α = 3.0 at T = 273 K and P_0 = 250 kPa) as an example.[85] The impurity concentration in the initial gas mixture was 3.5 mol.%.

Freon-12 is insoluble in water while SF_6 is water soluble, although poorly (solubility is 14.7 ml litre^{-1}). Therefore, separation of the components due to dissolution in water was ignored.

The experimental apparatus (Fig. 8) comprised three main units, *viz.*, a crystallizer, a thermostat and a gas inlet system. The thermostatted glass crystallizer (350 ml) was filled with distilled water by three-quarter volume. The external cooling jacket of the crystallizer was filled with cooling agent. The pressure in the crystallizer was controlled by a pressure vacuum gauge. The gas mixture under study was fed and removed using the gas inlet system which allowed one to evacuate the reactor, to feed the gas mixture and to perform sampling at any step of the experiment. A mixture of ethylene glycol (30%) with water (70%) was used as cooling agent. The thermostat maintained the temperature in the crystallizer in the range of 0 – 20 °C with an accuracy of ±0.5 °C. The experimental apparatus allowed one to study hydrate formation at pressures up to 300 kPa to an accuracy of ± 5 kPa.

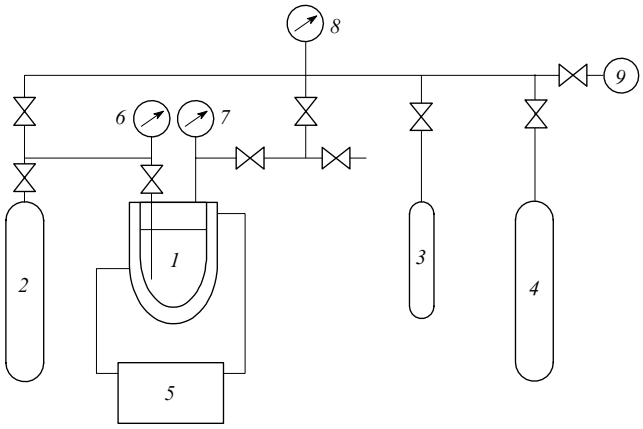


Figure 8. Design of experimental apparatus.[85]
Crystallizer (*1*), gas mixture bottle (*2*), sampling cylinder (*3*), helium container (*4*), thermostat (*5*), pressure vacuum gauges (*6*–*8*), and vacuum pump (*9*).

In carrying out gas hydrate crystallization under isobaric conditions, the constant pressure (P_0) in the crystallizer was maintained at 245 – 250 kPa. As the gas pressure in the crystallizer decreased by ΔP = 5 kPa upon the formation of gas hydrate, an additional portion of the gas mixture was fed into the system and the pressure returned to its initial value. The procedure was repeated several times; the sample ratio was determined from the equation

$$\theta = \frac{\sum \Delta P}{P_0 + \Delta P}\,. \tag{46}$$

The purified substance was sampled after the necessary value θ was reached.

In the second experimental regime, the initial pressure in the crystallizer was set to $P_0 = 250$ kPa. The formation of gas hydrate was accompanied by a decrease in the pressure in the crystallizer to P_k. In this case, the sample ratio was determined from the equation

$$\theta = \frac{P_0 - P_k}{P_0}. \tag{47}$$

As the necessary θ value was reached, the sample was transferred to a preliminarily mounted cylinder. The sample was diluted with helium and analyzed.

The experimental data are shown in Figs 9 and 10. As the sample ratio increases, the separation factor of the mixture increases; the experimental and theoretical values obtained using Eqns (40), (41) and (44), (45) are in good agreement.

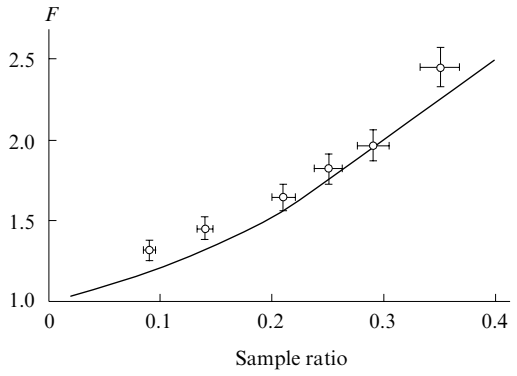


Figure 9. Separation factor of the mixture $SF_6-CF_2Cl_2$ plotted *vs.* sample ratio at constant pressure.[85]
Impurity concentration is 3.5 mol.%, $P_0 = 250$ kPa, $T = 273$ K. Here and in Fig. 10 open circles denote experimental data; the solid line represents the result of calculations using Eqns (40), (41) and (44), (45).

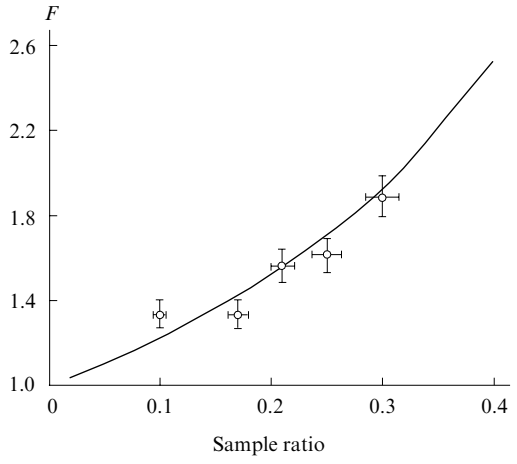


Figure 10. Separation factor of the mixture $SF_6-CF_2Cl_2$ plotted *vs.* sample ratio for directed crystallization.[85]
Impurity concentration is 3.5 mol.%, $T = 273$ K, $P_0 = 250$ kPa.

Based on the results of analysis (see above), one can suggest that the proposed mathematical model correctly describes experimental data and can be used for practical calculations of the separation factors of gas mixtures by the gas hydrate crystallization method.

5. Continuous gas hydrate crystallization

In the text above, we have considered gas hydrate crystallization at constant pressure with single separation of gas mixtures. But often, continuous separation and high purification of gas mixtures is needed. This requires practical implementation of continuous gas hydrate crystallization.[94, 96]

Consider the process of gas hydrate crystallization in a crystallizer at the interface at continuous flow rate of a gas mixture (Fig. 11).[94] The original gas mixture (flow rate l_0) is

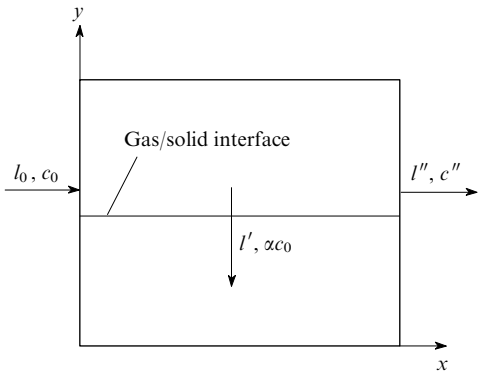


Figure 11. Separation of mixtures by continuous gas hydrate crystallization: a schematic.

fed along the interface. It is divided into two flows, namely, the crystallizable flow l' directed perpendicular to the interface and the flow l'' leaving the crystallizer along the x axis. The flow l' is determined by the crystallization rate and depends on the temperature and pressure in the system, on the concentration of the hydrate-forming gas and on the surface area of the gas–water contact. The fraction of the gas consumed in hydrate crystallization is given by

$$\eta = \frac{l'}{l_0} = 1 - \frac{l''}{l_0}. \tag{48}$$

Assuming that the impurity concentration in the gas mixture varies only along the x axis and that the flow l' does not vary with time, the mass balance equation for the impurity under steady flow conditions is as follows[94]

$$\frac{dc_i}{dt} = -\mathrm{div} J_i = 0, \tag{49}$$

where c_i is the impurity concentration in the gas flow and J_i is the mass flux of the impurity through the crystallizer.

After transformations, expression (49) takes the form

$$c\frac{dl}{dx} + l\frac{dc}{dx} = -\alpha c\frac{dl'}{dy}, \tag{50}$$

where α is the separation coefficient of the impurity; c is the impurity concentration in the gas mixture that is in equilibrium with the gas mixture in the hydrate; l is the gas flow rate at the point x.

The mass balance equation for the major component has the form

$$\frac{dc_1}{dt} = -\mathrm{div}J_1 = 0, \quad (51)$$

where c_1 is the concentration of the major component in the gas flow and J_1 is the mass flux of the major component through the crystallizer.

After rearrangements, expression (51) takes the form

$$\frac{dl'}{dy} = \frac{l}{1-c}\frac{dc}{dx} - \frac{dl}{dx}. \quad (52)$$

Simultaneous use of Eqns (49) and (52) gives:

$$c\frac{dl}{dx} + l\frac{dc}{dx} = -\alpha c\left(\frac{l}{1-c}\frac{dc}{dx} - \frac{dl}{dx}\right). \quad (53)$$

Solution of Eqn (53) by the method of separation of variables with the initial conditions $c = c_0$ and $l = l_0$ at $x = 0$ gives [94] the dependence of the impurity concentration in gas phase at the crystallizer outlet on the fraction of crystallized gas for a continuous process,

$$\left(\frac{c''}{c_0}\right)\left(\frac{1-c_0}{1-c''}\right)^{\alpha} = (1-\eta)^{\alpha-1}, \quad (54)$$

where c_0 and c'' are the initial and final impurity concentrations, respectively.

This mathematical model was used to calculate the dependence of the separation factor $F = c_0/c''$ on the sample ratio η for the mixture $SF_6 + SO_2$ (the separation coefficient $\alpha \approx 21.4$ at $T = 273$ K and $P_0 = 250$ kPa and the impurity concentration is 3.5%). The results of calculations are shown in Fig. 12. As can be seen, a large separation factor ($F > 100$) can be obtained even at low sample ratios (> 0.2).

As in the precedng case,[85] the proposed mathematical model for calculations of the efficiency of separation was verified taking the system sulfur hexafluoride – Freon-12 impurity (separation coefficient $\alpha \approx 3$ at $T = 273$ K, $P_0 = 205$ kPa) as an example.[94] The impurity concentration in the initial gas mixture was 3.5 mol.%.

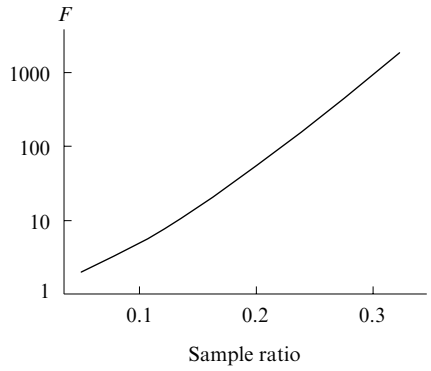


Figure 12. Separation factor of the mixture $SF_6 - SO_2$ plotted *vs.* sample ratio.[94]
SO_2 concentration is 3.5%, $T = 273$ K, $P_0 = 250$ kPa.

As mentioned above, continuous gas hydrate crystallization should be carried out under steady flow conditions l', *i.e.*, at constant crystallization rate. It was experimentally established that under the experimental conditions the maximum steady-state flow of 1.5 $cm^3\ min^{-1}$ was attained at least 150 min after the onset of crystallization.

To carry out continuous gas hydrate crystallization experiments on an apparatus described earlier,[85] the design of the crystallizer (*1*) (Fig. 13) was changed [94] to exclude mixing of the gas mixture in the reactor and to include rheometers at the crystallizer inlet and outlet (*2*, *3*) to determine the flow rate of the gas mixture. The flow was adjusted with a fine adjustment valve (*4*). The pressure in the crystallizer was set by the valve (*5*) and controlled by the pressure vacuum meter (*6*) with an accuracy to ± 5 kPa.

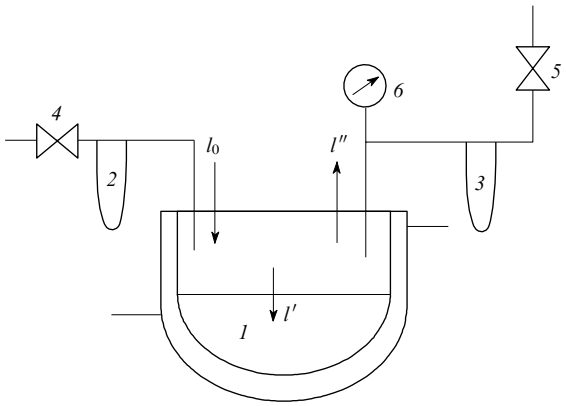


Figure 13. Design of experimental apparatus.[94]
Crystallizer (*1*); rheometers (*2*, *3*); valves (*4*, *6*); and pressure vacuum gauge (*6*).

The experimental apparatus allowed one to study crystallization at pressures up to 3 atm in the temperature range from 0 to 20 °C at gas flow rates up to 40 ml min^{-1}.

Gas hydrates were produced at constant pressure for 2 – 3 h to attain a constant crystallization rate. Then, the necessary sample ratio [see Eqn (48)] was set using the valves (*4*, *5*).

Sampling was carried out at a constant pressure of 250 kPa and different gas flow rates.

The concentration of the Freon-12 impurity in sulfur hexafluoride was determined by gas chromatography following a known procedure.[85] The results obtained are shown in Fig. 14. As can be seen, the separation factor of the mixture increases with an increase in the sample ratio and the results of calculations using Eqn (54) are in good agreement with experimental data.

Thus, the mathematical model described above correctly describes experimental data and can be used for practical calculations of the separation factor of gas mixtures by the continuous gas hydrate crystallization method. The technique enables highly efficient separation of gas mixtures and is suitable for purification of gases from impurities using simple equipment.

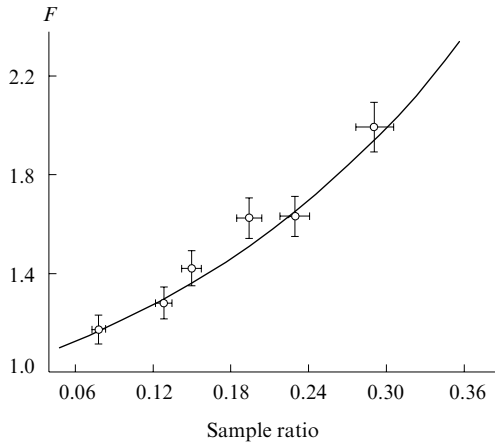


Figure 14. Separation factor of the mixture $SF_6-CF_2Cl_2$ plotted *vs*. sample ratio.[94]
CF_2Cl_2 concentration is 3.5%, $T = 273$ K, $P_0 = 250$ kPa. Open circles denote experimental data, the solid line represents the result of calculations using Eqn (54).

IV. High purification of fluorides by the gas hydrate crystallization method

Sulfur hexafluoride and carbon tetrafluoride are widely used in microelectronics for etching of boards. Continuous increase in the degree of integration of semiconductor microstructures leads to toughening of the requirements for the purity of substances. In some cases, traditional methods are inappropriate for the synthesis of substances with the desired purity. This gives an impetus to search for new approaches to the synthesis of high-purity substances. One of them can be the method based on the ability of CF_4 and SF_6 to form gas hydrates.

The possibility of using the gas hydrate crystallization method for purification of sulfur hexafluoride and carbon tetrafluoride was studied.[100–102] The relative distribution coefficients of the main impurities in binary gaseous systems 'major component–impurity' were calculated, different regimes of gas hydrate crystallization were considered and their efficiency in purification of gas mixtures was evaluated.

The following chemical compositions of impurities were reported in a monograph:[103]

for carbon tetrafluoride

N_2, O_2, CO_2, CF_2Cl_2, CH_4, SF_6, CHF_3, C_2F_6;

for sulfur hexafluoride

N_2, O_2, CO_2, SO_2.

All these impurities can form hydrates.

The gas hydrate crystallization of the systems based on CF_4 (SF_6) results in gas hydrates with the cubic structure I (II). The SF_6 molecules mainly occupy large cavities in the crystal framework because the Langmuir coefficient for the small cavity ($C_1 = 3.32 \times 10^{-5}$ kPa^{-1}) is smaller than for the large cavity ($C_2 = 7.51$ kPa^{-1}), but the CF_4 molecules occupy only large cavities ($C_2 = 2.79 \times 10^{-1}$ kPa^{-1}).

To calculate the Langmuir coefficients using Eqns (5), (7) and (8), the published values of the intermolecular interaction parameters for individual substances should be corrected. Therefore, the necessary values of the parameters for SF_6, O_2, N_2, CO_2, SO_2, CH_4 and CF_2Cl_2 were determined using the dissociation pressures and compositions of the corresponding individual gas hydrates using the procedure described by Avlonitis.[86] The error in determination was at most 3%. The Kihara potential parameters of pure individual substances thus obtained are listed in Table 5. Reliable data on the dissociation pressure of CF_4 hydrate are unavailable; therefore, the necessary values of the Kihara potential parameters were taken from Ref. 104. The dissociation pressure of individual CF_4 hydrate was determined using the theory of ideal solid clathrate provided that at the dissociation pressure, the water vapour pressure above the gas hydrate equals the saturated vapour pressure above water surface.[7] The dissociation pressure obtained was 325 kPa at 273.1 K.

Table 5. Kihara potential parameters for individual substances.[100]

Component	ε/k/K	σ/Å	a/Å	Component	ε/k, K	σ/Å	a/Å
SF_6	312	3.77	0.4	CO_2	213	3.58	0.27
CF_4	291	3.22	0.72	SO_2	360	3.42	0.35
O_2	164	3.3	0.18	CH_4 (see [a])	148.6	3.7	–
N_2	112.5	3.45	0.22	CF_2Cl_2	419.1	3.7	0.36

[a] Listed are the Lennard-Jones potential parameters.

The results of calculations of the relative distribution coefficient using Eqn (14) for impurities in the fluorides CF_4 and SF_6 subject to purification are listed in Table 6. As earlier,[81] the impurities for SF_6 can be divided into three groups. The first group of impurities includes CH_4, O_2 and N_2 characterized by $K_{21} < 1$. Small values of the relative distribution coefficients of these impurities are due to weak interaction between included gas molecules and water molecules from the crystal framework of gas hydrate. As a consequence, the Langmuir coefficients of these substances are small (about 10^{-4} kPa^{-1} for nitrogen and oxygen and about 10^{-3} kPa^{-1} for methane). Hence, the corresponding fractions of gas-filled cavities will be low. Consequently, in the formation of such gas hydrates, their cavities are mainly filled with the molecules of the major component, whereas the impurity remains in the gas phase. As the temperature increases, the relative distribution coefficients of these impurities in the CF_4 (SF_6) hydrate increase (decrease).

The second group of impurities includes CO_2 and SF_6 whose relative distribution coefficients are close to unity

Table 6. Theoretical values of the distribution coefficients for systems based on CF_4 (I) and SF_6 (II).[100]

Impurity [a]	I (see [b])	II (see [c])
CH_4	9.37×10^{-2}	–
O_2	2.48×10^{-2}	3.42×10^{-1}
N_2	1.59×10^{-2}	1.90×10^{-1}
CO_2	2.22×10^{-1}	1.47
SO_2	–	41.84
CF_2Cl_2	6.36	–
SF_6	1.28	–

[a] $c_0 = 1$ vol.%; [b] $P = 1000$ kPa, $T = 273$ K; [c] $P = 400$ kPa, $T = 273$ K.

due to larger values of the Langmuir coefficients. Carbon dioxide molecules ($C_1 \approx 10^{-3}$ kPa^{-1}, $C_2 \approx 10^{-1}$ kPa^{-1}) displace the SF_6 molecules ($C_1 = 3.32 \times 10^{-5}$ kPa^{-1}) from small cavities during the formation of gas hydrates in the system $SF_6 - CO_2$. However, since the SF_6 molecules mainly occupy large cavities in structure II and to a lesser extent small cavities, the relative distribution coefficient differs slightly from unity. It can become smaller than unity with a decrease in the pressure in the system. On the contrary, in the system $CF_4 - SF_6$, sulfur hexafluoride molecules ($C_2 = 4.59 \times 10^{-1}$ kPa^{-1}) displace the molecules of the major component from the large cavities in structure I, but since the Langmuir coefficients of the major component and impurity insignificantly differ from each other, the relative distribution coefficient also differs only slightly from unity.

The third group of impurities include SO_2 and CF_2Cl_2 whose relative distribution coefficients are larger than unity. Dichlorodifluromethane molecules occupy large cavities ($C_2 = 2.57$ kPa^{-1}) and displace carbon tetrafluoride molecules, whereas SO_2 molecules ($C_1 = 7.83 \times 10^{-2}$ kPa^{-1}) occupy small cavities in SF_6 hydrate. An increase in the temperature, pressure or impurity concentration in the system $CF_4 - CF_2Cl_2$ causes a noticeable decrease in the relative distribution coefficient.

Three regimes of gas hydrate crystallization in the systems based on CF_4 and SF_6 have been considered,[100] *viz*., directed crystallization, gas hydrate crystallization at constant pressure and continuous gas hydrate crystallization. To evaluate the efficiency of each regime, the dependences of the separation factor on the sample ratio were determined using Eqns (40), (41), (44), (45), (48) and (54). The impurities considered were CF_2Cl_2 and SF_6 in CF_4 as well as SO_2 and CO_2 in SF_6, *i.e*., all of them were crystallizable. The results of calculations are shown in Figs 15–18. In the case of gas hydrate crystallization at constant pressure, the separation factors of the impurities CF_2Cl_2, SF_6 and SO_2 tend to constant values as the sample ratio increases. The limiting attainable impurity concentration in the gas phase is determined by the c_0/A ratio [see Eqn. (40)].

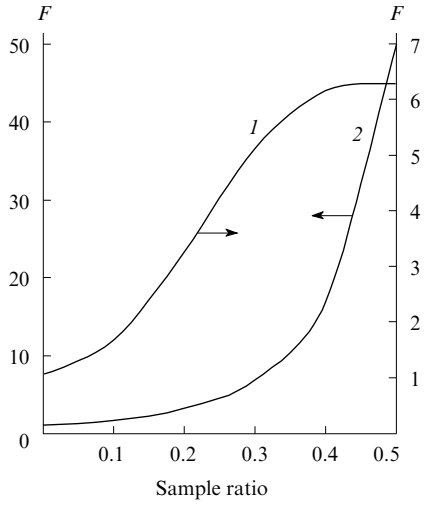


Figure 15. Plot of separation factor *vs*. sample ratio for the system $CF_4 - CF_2Cl_2$ at 273 K and 1000 kPa.[100]
Crystallization at constant pressure (*1*) and continuous and directed gas hydrate crystallization (*2*).

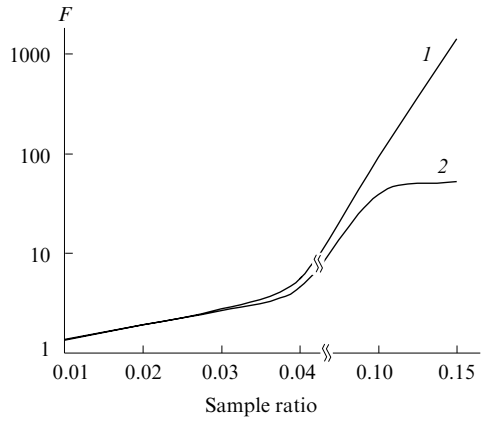


Figure 16. Separation factor plotted *vs*. sample ratio for the system $SF_6 - SO_2$ at 273 K and 400 kPa.[100]
Continuous and directed gas hydrate crystallization (*1*) and crystallization at constant pressure (*2*).

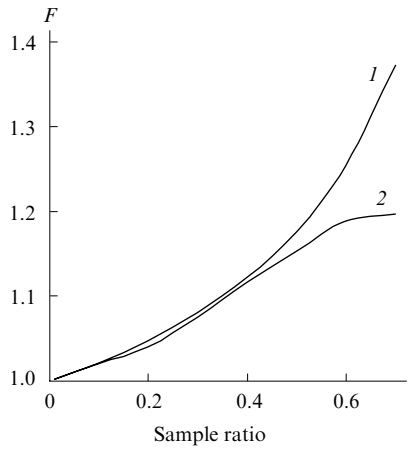


Figure 17. Separation factor plotted *vs*. sample ratio for the system $CF_4 - SF_6$ at 273 K and 1000 kPa.[100]
Continuous and directed gas hydrate crystallization (*1*) and crystallization at constant pressure (*2*).

As to continuous and directed gas hydrate crystallization, the separation factors of the impurities CF_2Cl_2 and SF_6 abruptly increase with an increase in the sample ratio (see Figs 15 and 17). Therefore, it is possible to obtain high separation factors for the components with large distribution coefficients at low sample ratios (< 0.1). In addition, the separation factors of all impurities considered are independent of the regime of gas hydrate crystallization at low sample ratios (see Fig. 16) and even at high sample ratios if the corresponding distribution coefficients are close to unity. Thus, in choosing the regime of purification of a gas mixture one should take into account only the components with high distribution coefficients (see Table 6).

For continuous and directed gas hydrate crystallization, the plot of the separation factor of CO_2 *vs*. sample ratio (see Fig. 18) passes through the point (1; 0) and reaches a maximum at a sample ratio of about 0.35. The appearance

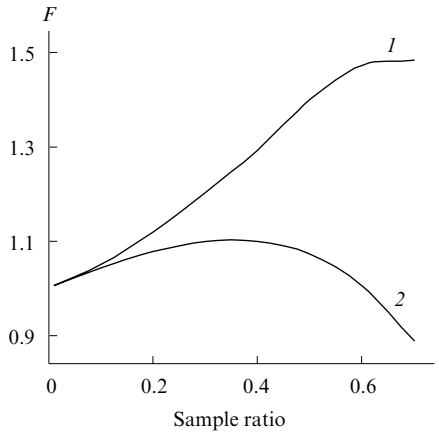


Figure 18. Separation factor plotted *vs.* sample ratio for system SF_6-CO_2 at 273 K and 400 kPa.[100]
Crystallization at constant pressure (*1*) and continuous and directed gas hydrate crystallization (*2*).

of maximum is due to the fact that as the sample ratio increases, the pressure in the system decreases, an additional portion of the substance is not supplied as in the case of crystallization at constant pressure and thus the relative distribution coefficient becomes less than unity.

Based on the results of analysis of the gas hydrate crystallization method, a procedure for high purification of sulfur hexafluoride was proposed.[100] It involves the gas hydrate crystallization method and two additional purification steps (Fig. 19). Gas hydrate crystallization is used as the first step. The impurities, CO_2 and SO_2, go from the gas phase to the solid phase. Since the gas subject to purification is saturated with water vapours during gas hydrate crystallization, they should be removed in some way. To this end, it was proposed to use cryofiltration through fibrous filters in the second step of purification. In the third step, it was proposed to use low-temperature distillation to remove the remaining impurities whose relative distribution coefficients are less than unity (*e.g.*, N_2 and O_2).

The concentrations of the main impurities in the initial sulfur hexafluoride and impurities in each step of purification and the compositions of the final products are listed in Table 7. It follows that the gas hydrate method of purification of sulfur hexafluoride allows one to obtain a product that meets modern requirements and is suitable for the use in electronic industry.

Table 7. Results of SF_6 purification by the gas hydrate crystallization method.[100]

Impurity	c_0 (vol.%)	c (vol.%)			c'' (vol.%)	γ (vol.%)
		step I	step II	step III		
N_2	0.02	0.025	–	1×10^{-3}	1×10^{-3}	6×10^{-3}
O_2	0.01	0.011	–	1×10^{-3}	1×10^{-3}	6×10^{-3}
CO_2	0.01	0.004	–	–	4×10^{-3}	4×10^{-3}
SO_2	0.01	2×10^{-4}	–	–	2×10^{-4}	3×10^{-3}
H_2O	0.0015	0.053	4×10^{-4}	–	4×10^{-4}	5×10^{-4}

Note. c_0, c and c'' are respectively the initial, running and final impurity concentrations; γ are the target values for the quality of SF_6 taken from Ref. 103.

Summing up, consideration of gas hydrate crystallization of SF_6 and CF_4 shows that such impurities as CO_2, SO_2 in the former and CF_2Cl_2, SF_6 in the latter case will crystallize as the corresponding gas hydrates. Other impurities studied will concentrate in the gas phase. Therefore, purification of SF_6 by the gas hydrate method combined with other highly efficient methods of high purification can extend the range of impurities that can be removed.

V. Conclusion

From the aforesaid it follows that the gas hydrate crystallization method can be successfully used for separation and high purification of substances.

The relative distribution coefficient for identical hydrate formation conditions strongly depends on the component ratio in the gas mixture and can in some cases be appreciably different from unity. Hence, during hydrate formation the major component can be considerably depleted or enriched in impurities. Separation of gas hydrates from the gas mixture allows one to purify the major component or to separate gas mixtures.

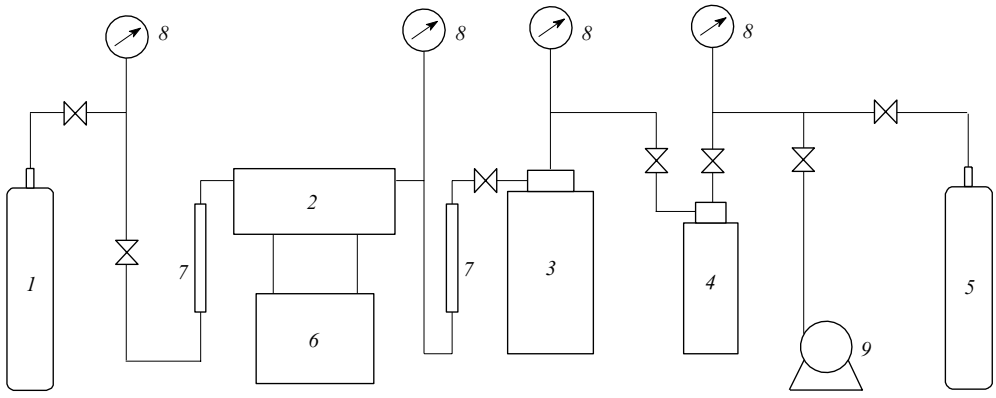


Figure 19. Apparatus for fine purification of sulfur hexafluoride: a schematic.[100]
Initial sulfur hexafluoride bottle (*1*), crystallizer (*2*), cryofilter and cryostat (*3*), distillation apparatus with a Dewar vessel (*4*), product container (*5*), thermostat (*6*), rotameters (*7*), pressure vacuum gauges (*8*) and vacuum pump (*9*).

Modern theoretical models for the formation of gas hydrates allow the distribution coefficients of molecules in the gas mixture in gas hydrate cavities to be calculated with a good accuracy.

The results of calculations show that modern mathematical models provide a reasonable description of high purification of substances by the gas hydrate crystallization method.

The formation of a nanosized phase during gas hydrate crystallization leads to significant redistribution of impurities between the gas and solid phases and can be used for separation and high purification of gases.

In addition, nanosized phases in the form of gas hydrates can be used for storage and transportation of gases. Data on redistribution of gaseous components in the formation of natural gas hydrates seem to be important taking into account the fact that such hydrates represent an inexhaustive source of hydrocarbon raw materials.[105–109]

Studies on separation of gases by the gas hydrate crystallization method revealed an important role of kinetic features of gas hydrate formation. The development of procedures to shorten the time necessary to form gas hydrates in the systems under study is also important.

It seems appropriate to extend the range of systems to be studied, *i.e.*, the number of substances capable of forming gas hydrates. At present, there are only a few such substances. However, some compounds form gas hydrates either at low temperatures or at elevated pressures and there is a need for the development of additional equipment for separation of gases by the gas hydrate crystallization method.

References

1. V M Vorotyntsev *Nanochastitsy v Dvukhfaznykh Sistemakh* (Nanoparticles in Two-Phase Systems) (Moscow: Izvestiya, 2010)
2. B A Nikitin *Izbrannye Trudy* (Selected Works) (Moscow: Academy of Sciences of the USSR, 1956)
3. V M Vorotyntsev, V M Malyshev *Russ. Chem. Rev.* **67** 81 (1998); *Usp. Khim.* **67** 87 (1998)
4. F A Kuznetsov, V A Istomin, T V Rodionova *Ros. Khim. Zh.* **47** (3) 5 (2003) [a]
5. C Y Sun, Q Huang, G J Chen *J. Chem. Ind. Eng.* **57** 1031 (2006)
6. A Klapproth, E Goreshnik, D Staykova, H Klein, W F Kuhs *Can. J. Phys.* (1–2) 503 (2003)
7. S Sh Byk, Yu F Makagon, V I Fomina *Gazovye Gidraty* (Gas Hydrates) (Moscow: Khimiya, 1980)
8. P Englezos *Ind. Eng. Chem. Res.* **32** 1251 (1993)
9. L F Smirnov *Zh. Prikl. Khim.* **65** (1) 138 (1992) [b]
10. L F Smirnov *Teoret. Osnovy Khim. Tekhnol.* (6) 808 (1989)
11. L A Kul'skii *Novye Metody Opresneniya Vody* (New Method of Water Desalination) (Kiev: Naukova Dumka, 1974)
12. L Z Mel'tser, L F Smirnov, in *Razlichnye Oblasti Primeneniya Kholoda* (Various Applications of Cold) (Moscow: Agropromizdat, 1985) p. 242
13. A J Barduhn *Chem. Eng. Prog.* **63** (1) 98 (1967)
14. L A Kul'skii, V V Dal' *Problemy Ochistki Vody* (The Problems of Water Desalination) (Kiev: Naukova Dumka, 1974)
15. US P. 6565715 (1999)
16. V A Istomin, V S Yakushev *Gaz. Prom-t' (Spets. Vyp.)* 56 (1996)
17. USSR P. 896854 ; *Byull. Izobret.* (44) (1983)
18. USSR P. 711758; *Byull. Izobret.* (3) (1980)
19. A Yu Manakov, Yu A Dyadin *Ros. Khim. Zh.* **47** (3) 28 (2003) [a]
20. Yu A Dyadin, in *XII Konkurs-konferentsiya im. Akademika A V Nikolaeva (Tezisy Dokladov)* [The XIIth Academician A V Nikolaev Competition-Conference (Abstracts of Reports), Novosibirsk, 2001] p. 54
21. I M Chou, A Sharma, R C Burruss, J F Shu, H K Mao, R J Hemley, A F Goncharov, L A Stern, S H Kirby *Proc. Natl. Acad. Sci. USA* **97** 13484 (2000)
22. A Yu Manakov, V I Voronin, A V Kurnosov, A E Teplykh, E G Larionov, Yu A Dyadin *Dokl. Akad. Nauk* **378** 503 (2001) [c]
23. A V Kurnosov, A Yu Manakov, V Yu Komarov, V I Voronin, A E Teplykh, Yu A Dyadin *Dokl. Akad. Nauk* **381** 649 (2001) [c]
24. V A Istomin, V S Yakushev *Gazovye Gidraty v Prirodnykh Usloviyakh* (Gas Hydrates in Natural Conditions) (Moscow: Nedra, 1992)
25. Yu A Dyadin, A L Gushchin *Soros. Obrazovat. Zh.* (3) 55 (1998) [d]
26. V I Kosyakov, V A Shestakov *Zh. Strukt. Khim.* **36** 495 (1995) [e]
27. S Sh Byk, V I Fomina, A F Narozhenko *Gaz. Prom-t'* (2) 35 (1971)
28. Yu F Makogon *Gidraty Prirodnykh Gazov* (Hydrates of Natural Gases) (Moscow: Nedra, 1974)
29. O B Kutergin, V P Mel'nikov, A N Nesterov *Dokl. Akad. Nauk* **323** 549 (1991) [c]
30. V M Vorotyntsev, V M Malyshev, in *Proceedings of the 2nd International Conference on Natural Gas Hydrates, Toulouse, 1996* p. 507
31. P Englezos, N Kalogerakis, P D Dholabhai *Chem. Eng. Sci.* **42** 2647 (1987)
32. P Skovborg, H J Ng, P Rasmussen, U Mohn *Chem. Eng. Sci.* **48** 445 (1993)
33. Y F Makogon, in *Fourth Canadian Permafrost Conference, 1981, Calgary, AB* (Ed. H M French) (Ottawa, ON: National Research Council of Canada, 1982) p. 299
34. P Bollavaram, S Devarakonda, M S Selim, E D Sloan *J. Phys. Chem.* **36** 1256 (1997)
35. P Y Zheng, S Y Wang, J D Shen, X He, F R Liu *Chem. Eng. (Chinese)* **33** (4) 26 (2005)
36. E D Sloan Jr *Clathrate Hydrates of Natural Gases* (New York: Marsel Dekker, 1990)
37. J H Van der Waals *Trans. Faraday Soc.* **52** 184 (1956)
38. R M Barrer, W J Stuart *Proc. R. Soc. London, Ser. A* **243** 172 (1957)
39. J H Van der Waals, J C Platteeuw *Adv. Chem. Phys.* **2** 1 (1959)
40. M I Shakhparonov *Vvedenie v Molekulyarnuyu Teoriyu Rastvorov* (Introduction to the Molecular Theory of Solutions) (Moscow: Gos. Izd. Tekhn.-Teoret. Lit., 1959)
41. L Lyndgaard, J H Molerup *Fluid Phase Equilib.* **70** 199 (1991)
42. R Rid, D Prausnits, T Shervud *Svoistva Gazov i Zhidkostei* (Properties of Gases and Liquids) (Leningrad: Khimiya, 1982)
43. Yu A Dyadin, K A Udachin, F V Zhurko *Izv. Sib. Otd. Akad. Nauk, Ser. Khim. Nauk* (1) 44 (1989)
44. V R Belosludov, M Y Lavrentiev, Y A Dyadin *J. Inclusion Phenom. Mol. Recognit. Chem.* **8** 59 (1990)
45. Yu A Dyadin, F V Zhurko, I V Bondaryuk *Klatratnye Gidraty pri Vysokikh Davleniyakh. Fazovye Diagrammy* (Clathrate Hydrates at High Pressures. Phase Diagrams) (Novosibirsk: Nauka, 1987)
46. V R Belosludov, M Yu Lavrent'ev, Yu A Dyadin *Teoriya Klatratov* (Theory of Clathrates) (Novosibirsk: Institute of Inorganic Chemistry, Siberian Branch of Academy of Sciences of USSR, 1988)

47. V A Istomin, in *Tekhnologiya Ekspluatatsii Gazokondensatnykh Mestorozhdenii Severa Tyumenskoi Oblasti: Sbornik Nauchnykh Trudov VNII Prirodnykh Gazov* (Development Processes of Gas-condensate Fields of the North of Tyumen Region: Proceedings of Research Institute of Natural Gases, Moscow, 1987) p. 88
48. G L Chen, T M Guo, in *Proceedings of the 2nd International Conference on Natural Gas Hydrates, Toulouse, 1996* p. 33
49. S-Y Lee, G D Holder *Roczn. Chem.* **49** 159 (1975)
50. V R Belosludov, Yu A Dyadin, O A Dracheva, G N Chekhova *Izv. Sib. Otd. Akad. Nauk, Ser. Khim. Nauk* (4) 60 (1979)
51. V R Belosludov, Yu A Dyadin, S I Fadeev *Izv. Sib. Otd. Akad. Nauk, Ser. Khim. Nauk* (3) 57 (1981)
52. V R Belosludov, Yu A Dyadin, G N Chekhova *Izv. Sib. Otd. Akad. Nauk, Ser. Khim. Nauk* (6) 58 (1983)
53. V R Belosludov, Yu A Dyadin, S I Fadeev, G N Chekhova, in *Termodinamicheskie Svoistva Rastvorov (Mezhvuzovskii Sbornik Nauchnykh Trudov)* [Thermodynamic Properties of Solutions (International Proceedings), Ivanovo, 1984] p. 56
54. V R Belosludov, Yu A Dyadin, M Yu Lavrent'ev *Teoreticheskie Modeli Klatratoobrazovaniya* (Theoretical Models of Clathrate-Formation) (Novosibirsk: Nauka, 1991)
55. V A Istomin *Zh. Fiz. Khim.* **61** 1404 (1987) [f]
56. S-Y Lee, G D Holder *AIChE J.* **48** 161 (2002)
57. B J Anderson, M Z Bazant, J W Tester, B L Trout *J. Phys. Chem. B* **109** 8153 (2005)
58. S J Wierzchowski, P A Monson *Ind. Eng. Chem. Res.* **45** 424 (2006)
59. S J Wierzchowski, P A Monson *J. Phys. Chem. B* **111** 7274 (2007)
60. A H Mohammadi, D Richon *Ind. Eng. Chem. Res.* **47** 1346 (2008)
61. A H Mohammadi, D Richon *Ind. Eng. Chem. Res.* **47** 451 (2008)
62. A H Mohammadi, D Richon *Ind. Eng. Chem. Res.* **47** 4966 (2008)
63. Y F Zhang, P G Debenedetti, R K Prud'homme, B A Pethica *J. Petrol. Sci. Eng.* **51** (1–2) 45 (2006)
64. A Bahadori, S Mokhatab, B F Towler *J. Nat. Gas Chem.* **16** 349 (2007)
65. J H Van der Vaals, J C Platteeuw *Mol. Phys.* **1** 91 (1958)
66. V T John, G D Holder *J. Phys. Chem.* **85** 1811 (1981)
67. V T John, G D Holder *J. Phys. Chem.* **86** 455 (1982)
68. V T John, G D Holder *J. Phys. Chem.* **89** 3279 (1985)
69. G D Holder, V T John *Fluid Phase Equilib.* **14** 353 (1983)
70. V M Vorotyntsev, V M Malyshev *Vysokochistye Veshchestva* (6) 50 (1993)
71. R M Barrer, A V J Edge *Proc. R. Soc. London, Ser. A* **300** 1 (1967)
72. V M Vorotyntsev, V M Malyshev *Vysokochis. Veshch.* (6) 89 (1994)
73. Z Youssef, A Barreau, P Mougin, J Jose, I Mokbel *Ind. Eng. Chem. Res.* **48** 4045 (2009)
74. D Kolesov, I Rokova, A Talis, I Yaminskii, G Tereshchenko *Nanoindustriya* (1) 20 (2010)
75. Y Seo, H Lee *Environ. Sci. Technol.* **35** 3386 (2001)
76. S P Kang, H Lee *Environ. Sci. Technol.* **34** 4397 (2000)
77. US P. 3097924 (1980)
78. V G Berezkin, E N Viktorova *Dokl. Akad. Nauk SSSR* **271** 1412 (1983) [c]
79. V M Vorotyntsev, V M Malyshev *Vysokochis. Veshch.* (2) 38 (1994)
80. V M Vorotyntsev, V M Malyshev *Zh. Fiz. Khim.* **73** 1892 (1999) [f]
81. V M Vorotyntsev, V M Malyshev, P G Taraburov *Zh. Fiz. Khim.* **75** 129 (2001) [f]
82. V M Vorotyntsev, V M Malyshev, P G Taraburov, in *The 13th International Conference of Crystal Growth in Conjunction with the Eleventh International Conference on Vapor Growth and Epitaxy, Kyoto, 2001* p. 377
83. V M Vorotyntsev, V M Malyshev, P G Taraburov, I V Kozyrev *Izv. Vyssh. Uchebn. Zaved., Khim. Khim. Tekhnol.* **47** (4) 122 (2004)
84. V M Vorotyntsev, V M Malyshev, P G Taraburov, I V Kozyrev, in *The 14th International Conference of Crystal Growth, Grenoble, 2004* p. 216
85. V M Vorotyntsev, V M Malyshev, G M Mochalov, P G Taraburov *Teor. Osnovy Khim. Tekhnol.* **35** 128 (2001) [g]
86. D Avlonitis *Chem. Eng. Sci.* **49** 1161 (1994)
87. M A Clarke, P R Bishnoi *Fluid Phase Equilib.* **211** (1) 51 (2003)
88. V M Vorotyntsev, V M Malyshev, P G Taraburov, I V Kozyrev *Zh. Fiz. Khim.* **78** 2035 (2004) [f]
89. V M Malyshev, P G Taraburov, I V Kozyrev, M V Zakharova, in *Tezisy Dokladov Mezhdunarodnoi Nauchnoi Konferentsii 'Kristallizatsiya v Nanosistemakh'* (Abstracts of Reports of International Research Conference 'Crystallization in Nanosystems', Ivanovo, 2002) p. 127
90. V I Kosyakov, V A Shestakov *Zh. Fiz. Khim.* **72** 1951 (1998) [f]
91. V I Kosyakov, V A Shestakov *Dokl. Akad. Nauk* **348** 488 (1996) [c]
92. V I Kosyakov, V A Shestakov *Zh. Strukt. Khim.* **37** 916 (1996) [e]
93. V M Vorotyntsev, V M Malyshev *Dokl. Akad. Nauk* **372** 192 (2000) [c]
94. V M Vorotyntsev, V M Malyshev, G M Mochalov, P G Taraburov *Teor. Osnovy Khim. Tekhnol.* **35** 513 (2001) [g]
95. V M Vorotyntsev, V M Malyshev, P G Taraburov, I V Kozyrev, in *Tezisy Dokladov Mezhdunarodnoi Nauchnoi Konferentsii 'Kristallizatsiya v Nanosistemakh'* (Abstracts of Reports of International Research Conference 'Crystallization in Nanosystems', Ivanovo, 2002) p. 29
96. V M Vorotyntsev, V M Malyshev, P G Taraburov, in *The 13th International Conference of Crystal Growth in Conjunction with the Eleventh International Conference on Vapor Growth and Epitaxy, Kyoto, 2001* p. 515
97. V M Vorotyntsev, V M Malyshev, P G Taraburov, I V Kozyrev, in *Proccedings of the 16th Symposium of Industrial Crystallization, Dresden, Germany, 2005* p. 951
98. V M Vorotyntsev, V M Malyshev, in *Tezisy Dokladov VI Mezhdunarodnoi Nauchnoi Konferentsii 'Kinetika i Mekhanizm Kristallizatsii. Samoorganizatsiya pri Fazoobrazovanii'* (Abstracts of Reports of the International Research Conference 'Kinetics and Mechanism of Crystallization. Self-Organization in Phase-Formation', Ivanovo, 2010) p. 146
99. V M Vorotyntsev, V A Perevozchikov, V D Skupov *Bazovye Protsessy Mikro- i Nanotekhnologii. Uchebnoe Posobie* (Base Processes of Micro- and Nanotechnology. Study Book) (Nizhnii Novgorod: Nizhnii Novgorod State University, 2006)
100. V M Malyshev, P G Taraburov, I V Kozyrev *Izv. Akad. Inzh. Nauk im. A M Prokhorova* **7** 134 (2004)
101. V M Vorotyntsev, V M Malyshev, G M Mochalov, P G Taraburov, I V Kozyrev, S S Suvorov, in *Tezisy Dkladov XVII Mendeleevskogo S"ezda po Obshchei i Prikladnoi Khimii* (Abstracts of Reports of the XVIIth Mendeleev Congress on General and Applied Chemistry, Kazan, 2003) Vol. 2, p. 310
102. V M Vorotyntsev, V M Malyshev, P G Taraburov, I V Kozyrev, in *Proccedings of the 16th Symposium of Industrial Crystallization, Dresden, Germany, 2005* p. 1165

103. B N Maksimov, V G Barabanov, I L Serushkin, V S Zotnikov, I A Semerikova, V P Stepanov, N G Sagaidakova, G I Kaurova *Promyshlennye Ftororganicheskie Produkty* (Industrial Organofluorine Products) (St Petersburg: Khimiya, 1996)
104. V McKoy, O Sinanoglu *J. Chem. Phys.* **38** 317 (1963)
105. F A Kuznetsov, Yu A Dyadin, T V Rodionova *Ros. Khim. Zh.* **41** (6) 28 (1997) [a]
106. V S Yakushev, E V Perlova, V A Istomin, V A Kuz'minov, N N Solov'ev, L S Salina, N A Makhonina, S A Leonov *Resursy i Perspektivy Osvoeniya Netraditsionnykh Istochnikov Gaza v Rossii* (Resources and Prospects of Development of Nontraditional Sources of Gas in Russia) (Moscow: IRTs Gazprom, 2007)
107. J J Cerroll *Natural Gas Hydrates: A Guide for Engineers* (Amsterdam: Elsevier, Gulf Professional Publ., 2003)
108. B F Towler, S Mokhatab *Hydrocarb. Proc.* **84** (4) 61 (2005)
109. Yu F Makogon *Gaz. Prom-t'* (5) 10 (2001)

[a] — *Mendeleev Chem. J. (Engl. Transl.)*
[b] — *Russ. J. Appl. Chem. (Engl. Transl.)*
[c] — *Dokl. Phys. Chem. (Engl. Transl.)*
[d] — *Soros Educ. J. (Engl. Transl.)*
[e] — *J. Struct. Chem. (Engl. Transl.)*
[f] — *Russ. J. Phys. Chem., Ser. A (Engl. Transl.)*
[g] — *Theor. Found. Chem. Eng. (Engl. Transl.)*